T.C.

YEDITEPE UNIVERSITY

INSTITUTE OF HEALTH SCIENCES

DEPARTMENT OF PHARMACEUTICAL TECHNOLOGY

THREE-DIMENSIONAL PRINTING OF ANTIDIABETIC TABLETS

AHMED MOHAMMED WADI WADI, MSc

ISTANBUL-2021

T.C.

YEDITEPE UNIVERSITY

INSTITUTE OF HEALTH SCIENCES

DEPARTMENT OF PHARMACEUTICAL TECHNOLOGY

DRUG AND COSMETICS PRODUCTION TECHNOLOGIES PROGRAM

THREE-DIMENSIONAL PRINTING OF ANTIDIABETIC TABLETS

AHMED MOHAMMED WADI WADI, MSc

ADVISOR

Assist. Prof. Dr. Muhammed Abdur RAUF

ISTANBUL-2021

THESIS APPROVAL FORM

Institute : Yeditepe University Institute of Health Sciences

Program : Master in Drug and Cosmetics Production Technologies

Title of the Thesis : Three-Dimensional Printing of Antidiabetic Tablets

Owner of the Thesis : Ahmed Mohammed Wadi, MSc.

Examination Date : 30.06.2021

This study has been approved in content and quality by the Jury as a Master Thesis.

	Title, Name-Surname (Institution)
Chair of the Jury:	Prof.Dr. İmran VURAL, Hacettepe University
Advisor:	Assist.Prof.Dr. Muhammed Abdur RAUF, Yeditepe University
Member/Examiner:	Prof.Dr. Çetin TAŞ, Yeditepe University

APPROVAL

This thesis has been deemed appropriate by the above jury in accordance with the relevant articles of Yeditepe University Graduate Education and Examinations Regulation and has been approved by Institute Administrative Board with decision dated ..... and numbered .....

Prof. Dr. Bayram YILMAZ

Director of Institute of Health Sciences

DECLARATION

I hereby declare that this thesis is my own work and that, to the best of my knowledge and belief, it contains no material previously published or written by another person nor material which has been accepted for the award of any other degree except where due acknowledgment has been made in the text.

Date : 30.06.2021

Name Surname : Ahmed Mohammed Wadi

DEDICATION

To my dear Parents and Sisters…

ACKNOWLEDGEMENTS

I would like to express my sincere thanks to my advisor Dr. Muhammed Abdur Rauf for his interest in this study, and whose continues guidance and support cannot be overestimated.

I am deeply thankful to Prof. Dr. Çetin Taş for his valuable advices and profound insight. This project wouldn't have been possible without the help and tremendous hospitality of Genetics and Bioengineering Department vice chair Prof. Dr. Gamze Kose, who welcomed us in her laboratory and have been very tolerant and hospital to our long hours of 3D printing sessions. I would also like to extend my gratitude to Dr. Ebru Acar and Dr. Esra Bayram from the Faculty of Pharmacy for always having their door open for consultants in science and research life and setting an example for me of what an academic can be.

I would like to recognize the assistance of my colleague and dear friend Burcu Üner for being exceedingly patient in helping me navigate the different equipment and laboratories. I'd like to also acknowledge the constant help of our department assistance Bilal Şenkal, our 3DP technicians Beyza Mat and Özlem Beydilli.

Last but not least, I am deeply grateful for the support, patience and love of my family and my dear close friends Ahmed, Kira and Khaldun. And I don't forget Uysal and Elif.

TABLE OF CONTENTS

APPROVAL	ii
DECLARATION	iii
DEDICATION	iv
ACKNOWLEDGEMENTS	v
TABLE of CONTENTS	vi
LIST OF TABLES	ix
LIST OF FIGURES	x
LIST OF SYMBOLS AND ABBREVIATIONS	xii
ABSTRACT	xiii
ABSTRACT (Turkish)	xiv
1. INTRODUCTION AND PURPOSE	1
2. LITERATURE REVIEW	3
2.1. Personalized Therapy	3
2.2. Repaglinide	4
2.3. Three-Dimensional Printing	5
2.3.1. Brief History on Three-Dimensional Printing	5
2.3.2. Classification of Three-Dimensional Printing Technologies	7
2.3.3. Applications of 3DP within the Pharmaceutical Field	10
2.3.4. Bioplotter and How It Works	16
3. MATERIALS AND METHODS	22
3.1. Materials	22
3.2. Equipment	23
3.3. Methods	24
3.3.1. Identification of Repaglinide Using ATR-FTIR Spectroscopy/DSC	24
3.3.2. HPLC Analytical Method for the Quantification of Repaglinide	24
3.3.3. Digital Design of the Perforated Tablets	26
3.3.4. Preparation of the Binder Gel	27

3.3.5. Preparation of the Printing Ink/Paste 28
3.3.6. Semi-Solid Extrusion Printing of the Tablets 29
3.3.7. Evaluation of the Printed Tablets 29
3.3.8. Comparison of Dissolution Profiles 31
3.3.9. Modelling of the Drug Release Kinetics 32
3.3.10. Assessment of Drug-Excipient Interaction 33
4. RESULTS 34
4.1. Identification of Repaglinide using ATR-FTIR/DSC 34
4.2. Quantitative Determination of Repaglinide by HPLC 35
4.2.1. Repaglinide Calibration Curve 36
4.2.2. Validation of Analytical Method for Repaglinide 37
4.3. Three-dimensional Printed Tablets 39
4.4. Evaluation of the Printed Tablets 41
4.4.1. Size and Hardness 42
4.4.2. Weight Variation 43
4.4.3. Friability 44
4.4.4. Drug Content 45
4.4.5. Scanning Electron Microscopy (SEM) 46
4.4.6. Dissolution Study 46
4.4.7. Comparison of Dissolution Profiles 48
4.4.8. Modelling of Drug Release Kinetics 50
4.4.9. Two-Way Analysis of Variance ANOVA 50
4.4.10. Assessment of Drug-Excipient Interactions 50
5. DISCUSSION AND CONCLUSION 52
5.1. Identification of Repaglinide using ATR-FTIR 52
5.2. Optimizing of Printing Ink/ Paste 52
5.3. Evaluative Studies on Tablets 56
5.3.1. Hardness 56
5.3.2. Weight Variation 57
5.3.3. Friability 58

5.3.4. Thickness and Diameter 58
5.3.5. Dissolution and Release 59
5.3.6. Comparison of Dissolution Profiles 61
5.3.7. Modelling of Drug Release Kinetics 63
5.3.8. Assessment of Drug-Excipient Interactions 64
5.4. Conclusion 65
6. REFERENCES 66

LIST OF TABLES

Table 3.1. List of materials 22

Table 3.2. List of equipment 23

Table 3.3. Composition of the printing ink/paste 28

Table 4.1. Linear regression data (n=6) obtained in HPLC analysis of Repaglinide 36

Table 4.2. Intra-day and inter-day accuracy and precision 38

Table 4.3. Size values of the tablets (Thickness and Diameter) 41

Table 4.4. Hardness values of tablets in Kilopond (Kp) 42

Table 4.5. Weight values of the tablets 43

Table 4.6. Friability results of the tablets 44

Table 4.7. Drug Content values for 10 samples of each formulation. 45

Table 4.8. Similarity and difference factor values for different pairs of tablets 49

Table 4.9. Dissolution efficiency (%), AUCs (%-h) and comparison of AUCs 49

Table 4.10. Korsmeyer-Peppas model fit date and the predicted release mechanism 50

Table 4.11. Two-Way ANOVA results of perforation and formulation 50

LIST OF FIGURES

Figure 2.1. The various 3D printing technologies mechanism 10

Figure 2.2. Example of pharmaceutical dosage forms developed by different 3D printing technologies 11

Figure 2.3. Channeled tablets to accelerate disintegration drug release from IR formulation 12

Figure 2.4. 3D printed Paracetamol tablet of different shapes with diverse release profile 12

Figure 2.5. (a.) 3D tablets of similar ratio (SA/V), (b.) 3D tablets of different (SA/V) ratio; SA/V = Surface area to volume 13

Figure 2.6. 3D printed Isoniazid tablet of varying size/dose (a.) Digital model (b.) tablets and filament 13

Figure 2.7. 3D printed Polypill, consisting of multiple compartments of different drugs for immediate and sustained release 14

Figure 2.8. Multi-compartmental 3D printed tablet against cardiovascular diseases, containing different drugs for early and sustained release 15

Figure 2.9. 3D printed capsular devise for timed pulsatile release (A) actual tablet (B) timed images of tablet in dissolution test 15

Figure 2.10. 3D role in promoting personalized therapy from 16

Figure 2.11. EnvisionTEC Bioplotter (Developer Series) 17

Figure 2.12. Loaded cartridges equipped with blunger and a needle 18

Figure 2.13. Loaded cartridge fitted inside the low temperature modular head 19

Figure 2.14. Modular heads types and specifications 20

Figure 2.15. Filling patterns available for the Bioplotter (EnvisionTEC) 21

Figure 3.1. Illustration of tablet digital design: (a) 1.0SD, (b.) 1.3SD, (c.) 1.6SD 27

Figure 3.2. Preparation of the binder gel from (54). 28

Figure 4.1. ATR-FTIR spectrum of pure repaglinide (a) obtained from our API using our machine (b.) obtained from literature (Olteanu et al., 2014). 34

Figure 4.2. Differential scanning calorimetry thermogram for repaglinide 35

Figure 4.3 HPLC chromatogram of repaglinide in mobile phase (2.5µg/mL) 36

Figure 4.4. Calibration curve of repaglinide in mobile phase and regression equation 37

Figure 4.5. Inter-day accuracy lines (n=3) three consecutive days 38

Figure 4.6. HPLC graph of Drug-free formulation (top), and Drug-loaded (bottom) 39

Figure 4.7. Top View of the 3D printed tablets 40

Figure 4.8. Horizontal view of the 3D printed tablets 40

Figure 4.9. Box plot summary of tablet thickness (mm) 41

Figure 4.10. Box plot summary of tablet Diameter (mm) 42

Figure. 4.11. Box plot summary of hardness values 43

Figure 4.12. Box plot summary of weight values (mg) 44

Figure 4.13. Box plot summary of friability values 45

Figure 4.14. SEM images of the 3D printed tablets 46

Figure 4.15. Release profile of 100K formulation (n=3) ± SD 47

Figure. 4.16. Release profile of 15K formulation (n=3) ± SD 47

Figure 4.17. Release profiles of the 6 tablets (n=3) 48

Figure 4.18. Thermogram of 15K HPMC formulations; mix 3 drug-free tablet, mix 4 drug-loaded tablet 51

Figure 4.19. Thermograms of100K HPMC formulations; mix 1 drug-free tablet, mix 2 drug-loaded tablet 51

Figure 5.1. 3D printed tablet of crumbling cone-like shape due to the softness of paste/ink 53

Figure 5.2. Inconsistent strand diameter attributed to poor hydration of paste 54

Figure 5.3. Image of the tablets resulting from the gradual experimental optimization of paste/ink and printing settings (top view) 55

Figure 5.4. Image of the tablets resulting from the gradual experimental optimization of paste/ink and printing settings (side view) 56

Figure 5.5. Weight of tablets plotted against hardness values. 57

Figure 5.6. Visual comparison of the different mechanical attributes of the 3D printed tablet 59

LIST OF SYMBOLS AND ABBREVIATIONS

3DP	Three-dimensional printing
AM	Additive manufacturing
EBP	Extrusion based printing
SSE	Semi-solid extrusion
API	Active pharmaceutical ingredient
BCS	Biopharmaceutics Classification System
CAD	Computed aided design
DOD	Drop on drop
DOS	Drop on solid
FDA	Food and Drug Administration
FDM	Fused deposition modeling
HME	Hot melt extrusion
HPMC	Hydroxypropyl methylcellulose
ODF	Orodispersible films
PEG	Poly(ethylene glycol)
PLA	Polylactic acid
PVA	Poly(vinyl alcohol)
PVP	Polyvinylpyrrolidone
RP	Rapid prototyping
SD	Strand Distance
SLA	Stereolithography
SLM	Selective laser melting
SLS	Selective laser sintering
T2DM	Type 2 Diabetes Meletus
FTIR-ATR	Fourier Transform Infrared - Attenuated Total Reflectance
DSC	Differential Scanning Calorimetry

ABSTRACT

Wadi, AM. (2021). Three-Dimensional Printing of Antidiabetic Tablets. Yeditepe University Institute of Health Sciences, Drug and Cosmetics Production Technologies, Istanbul. This study was conducted to employ the novel technology of three-dimensional printing as an alternative to conventional tableting technology in order to produce geometrically customizable tablet that offers personalized and tunable release profile. In addition to customization of release profile, geometrical design was utilized to enhance the dissolution of poorly water-soluble drug repaglinide from tablet dosage form. Semi-solid extrusion with a three-dimentional (3D) bioprinting machine (EnvisionTEC Bioplotter, Germany) was used as the production technology. Paste of traditional pharmaceutical excipients was formed by mixing powdered component and adding liquid binder. Lactose was used as a filler, PEG 6000 as a plasticizer, while different viscosity grades of hydroxypropylmethyl cellulose (HPMC,100K, and 15K mPa.s) served as release modifier polymers. Repaglinide was the antidiabetic active pharmaceutical ingredient (API) and the model for poorly water-soluble BCS class II drug. The liquid binder was formed as 0.5 % (w/v) gel of HPMC E4M in water, and added in a sufficient amount to create an extrudable, printable paste through a 0.41 mm nozzle. The tablets digital cylindrical design was created using Prefactory® RP program (EnvisionTEC, Germany), and then it was exported to the printer operating program VisualMachines. Two separate formulations were developed using HPMC 100K mPa.s and HPMC 15K mPa.s and, within each formulation, three different types of tablets were printed with strands distances (SD) parameter of 1.0, 1.3, and 1.6 mm (which determined the perforation levels within tablets). The resulting tablets were evaluated by their thickness, diameter, hardness, weight variation, friability, and dissolution profiles. The difference in these attributes were investigated in relation to their HPMC grades and 3D printing SD parameter. Overall, higher perforation levels in tablets and lower viscosity grades of HPMC produced higher rates of dissolution. Additionally, controlling perforations was also successful in enhancing the dissolution of the poorly water-soluble drug repaglinide. Hence, 3DP can be used to design tablets with customized release profiles to suit personalized medication with a 3D printer in clinical settings such as pharmacies and hospitals.

Key Words: 3D Printing, repaglinide tablet, personalized therapy, drug release, dissolution enhancement

ÖZET

Wadi, AM. (2021). Antidiyabetik Tabletlerin Üç Boyutlu Basımı. **Yeditepe Üniversitesi Sağlık Bilimleri Enstitüsü, İlaç ve Kozmetik Üretim Teknolojileri, İstanbul.**

Bu çalışma, kişiselleştirilmiş, ayarlanabilir ilaç salınım profili sunan geometrik olarak özelleştirilebilir tablet üretmek için geleneksel tablet basma teknolojisine alternatif olarak yeni üç boyutlu baskı teknolojisini kullanmak için yapılmıştır. Salım profilinin özelleştirilmesine ek olarak, suda çok az çözünen ilaç repaglinid'inin tablet dozaj formundan çözünmesini arttırmak için geometrik tasarım kullanılmıştır. Üretim teknolojisi olarak üç boyutlu (3D) biyo-yazıcı (EnvisionTEC Bioplotter, Almanya) ile yarı katı ekstrüzyon tekniği kullanılmıştır. Toz halindeki geleneksel farmasötik eksipiyan karışıma sıvı bağlayıcı eklenerek ekstrüzyon için uygun yarı katı hali oluşturulmuştur. Dolgu maddesi olarak laktoz, plastikleştirici olarak PEG 6000 kullanılırken, farklı viskozite dereceli hidroksipropilmetil selüloz (HPMC 100K ve 15K mPa.s) salınım değiştirici polimer olarak kullanılmıştır. Suda çok az çözünen, BCS sınıf II ilacının model olarak antidiyabetik aktif farmasötik bileşen (API) repaglinid kullanılmıştır. Sıvı bağlayıcı, su içinde %0.5 (a/h) HPMC E4M jel olarak oluşturulmuş ve 0,41 mm nozılden ekstrüde edilebilir, yazdırılabilir bir yarı katı karışımı oluşturmak için yeterli miktarda ilave edilmiştir. Tabletlerin dijital silindirik tasarımı Prefactory® RP programı (EnvisionTEC, Almanya) kullanılarak oluşturulmuş, ardından yazıcı işletim programı VisualMachines'e aktarılmıştır. HPMC100K mPa.s ve HPMC 15K mPa.s kullanılarak iki ayrı formülasyon geliştirilmiş ve her formülasyon içinde tabletlerdeki perforasyon seviyelerini belirleyen 1.0, 1.3, and 1.6 mm SD parametreli 3 farklı tipte tablet basılmıştır. Elde edilen tabletler kalınlık, çap, sertlik, ağırlık değişimi, sürtünme kontrolları ve çözünme profilleri ile değerlendirilmiştir. Bu özniteliklerdeki farkları, HPMC çeşidi ve 3D baskı parametreleri (SD) ile ilgili olarak araştırılmıştır. Genel olarak, tabletlerde daha yüksek perforasyon seviyeleri ve HPMC'nin daha düşük viskozite dereceleri, daha yüksek çözünme oranlarını göstermiştir. Ek olarak, perforasyonun kontrol edilmesi, suda az çözünen ilaç repaglinid'inin çözünmesini arttırmada da başarılı olmuştur. Bu nedenle, eczaneler ve hastaneler gibi klinik ortamlarda bir 3D yazıcı ile özelleştirilmiş salınım profillerine sahip tabletler tasarlayarak kişiselleştirilmiş tedavi için kullanılabilir.

Anahtar Kelimeler: 3D yazıcı, repaglinid tablet, kişiselleştirilmiş terapi, ilaç salınım, çözünme artırma

1. INTRODUCTION AND PURPOSE

The subject of this study is to successfully prepare printable paste/ink of traditional pharmaceutical excipients and, using three-dimensional printing technology (3DP), print sustained release tablets of the poorly water-soluble drug repaglinide. Repaglinide is an antidiabetic drug that is available commercially in immediate release tablet form only. This study will also demonstrate 3DP as a tool for personalized therapy.

Three-dimensional printing (3DP) is the technology of fabricating 3D object by subsequent deposition of layers of materials. 3DP first emerged as a prototyping technology but soon found application in all kind of industries. Three-dimensional Printing applications within the pharmaceutical dosage form production is a new and attractive frontier that is increasingly researched. It was employed in production of various dosage forms such as multi-compartmental capsules (1), orodispersable films (2), Intrauterine devices (3-4), vaginal rings (5), orally disintegrated (6), and swallowable tablets (7-8) among other applications.

3DP has been proposed as a new and innovative technology to produce personalized dosage forms, that is tailored to each patient specifically. It takes into account their induvial variation, needs, and aim of therapy (9).

Repaglinide was found to have high lipophilicity (Log *P* value of 3.97) and low solubility of 34 µg/ mL (10). This makes repaglinide a Biopharmaceutical Classification System Class II drug, that means repaglinide possess high permeability (which allows it to be readily absorbed through the gastrointestinal tract), and low solubility (which governs its dissolution from tablet dosage forms). Repaglinide possess limited oral bioavailability < 55% which is attributed in part to its poor solubility along with its high first-pass hepatic metabolism (11).

In this thesis we aim to:

- Propose 3DP as viable technology to improve dissolution of poorly water-soluble drugs through tablet design fabrication, for this purpose repaglinide serves as a model for BCS class II molecule

- Design diverse graded release profiles by control of tablet filling design as well as formulation. Ultimately, to be able to design a target release profile
- Explore 3DP as a feasible method in producing complex, and personalized release tablet dosage forms.
- Use the capability of 3DP to design a synergistic multi-drug antidiabetic tablet of repaglinide and metformin

2. LITERATURE REVIEW

2.1. Personalized Therapy

Personalized therapy can be defined as tailoring of medication for the specific need of an individual patient (12). The pharmaceutical industry produces medications in "one size fit all" model, where everyone gets the same dose, shape and mode of release of the medication.

Individual variation among patients creates diverse response to same medication treatment. These individual needs cannot be met by traditional pharmaceutical mass production and must be satisfied with more personalized medication.

Chronic disease, especially progressive chronic diseases such as diabetes mellitus and cardiovascular diseases are one of the major motives calling, and can benefit greatly from personalized therapy. These diseases, with time, progress in their pathology and require constant monitoring and subsequent adjustment of their treatment. These changes are very specific in nature to each patient.

Type 2 Diabetes mellitus (T2DM) is a chronic progressive disease caused by impaired insulin secretion from pancreatic β-cells and/or resistance to insulin. Nevertheless, T2DM is characterized by complex pathology where environmental and genetic factors are responsible for the pathophysiological abnormalities that ultimately results in impaired glucose homeostasis and elevated blood glucose levels (13). These environmental and genetic Individual factors such as age, sex, weight, pregnancy, hormones and genetic predisposition as well as comorbid diseases and other medication intake play a major role in the incidence of the disease as well as the response to the treatment. Optimal Treatment of T2DM requires careful consideration of all these factors, constant monitoring of disease progression (through tests such as fasting blood glucose and HBA1C1) and the relevant adjustment and personalization of treatment. The American Diabetes Association releases its annual diabetes mellitus management guidelines which takes into account, and design separate guidelines for the diverse demography of T2DM.

In 2015, the United States launched the precision medicine research initiative which is aimed at accelerating development in personalized therapy that takes into account the individual variation of the patients in order to enhance prevention and treatment of diseases such as cancer and diabetes (14). The individual variation presents among the different patients such as dietary habit, figures, living environment, sex, and genetic makeup govern a person's risk of developing a disease, as well as, the mode and severity of progression, and the individual response to treatment (15-17).

Three-dimensional printing has been a promising technology for personalized therapy (18), due to the flexibility it provides in controlling morphology, size, and percentage of API in dosage forms.

It can create dosage forms with diverse release behavior through its precise and minute ability to fabricate geometry (19). Tablets of enhanced palatability and unique candy-like shape were printed aimed to appeal to pediatrics patients between the age of 2 – 11 years old (20). Goyanes et al. demonstrated excellent linear relationship between tablet infill and API dose, showing that dosage can be controlled through geometry (21). More on 3DP application in pharmaceutical dosage form production and personalized therapy in section 2.3.3.

2.2. Repaglinide

Repaglinide is an oral anti-diabetic drug used to for the treatment of type 2 diabetes mellitus, it normalizes postprandial blood glucose through stimulation of insulin release from pancreatic β-cells (22).

Repaglinide is administered 0.5- 4 mg, 30 minutes prior to meal twice to 3 times daily with a maximum dose of 16 mg. dosage is titrated according to efficacy and patient response, which is evaluated through monitoring of HBA1c and fasting glucose levels. Monitoring fasting glucose levels should starts as early as one week after the start of the treatment (23).

Study on lipophilicity and solubility of repaglinide shows that is poses high lipophilicity (Log *P* value of 3.97) and low solubility of 34 µg/mL at 37 °C (10). This makes repaglinide a classic (Biopharmaceutical Classification System Class II (BCS II)

molecule. Despite the high lipophilicity of repaglinide which grants it high absorption through the gastrointestinal tract, repaglinide suffers from low oral bioavailability (< 55%) (11). This is attributed in part to its low solubility which results in its poor dissolution. Researches has been conducted aiming to improve the solubility and dissolution of repaglinide; Li-Fang Yin et al. enhanced the solubility and subsequently the dissolution of repaglinide by formulating a solid dispersion using polyvinylpyrrolidone as a carrier (24). Nanoemulsions systems of repaglinide were developed (25-26). Meglumine in 50% (v/v) ethanol was used to dissolve repaglinide in order to improve in vitro dissolution of tablets (27).

In our study, we aim to enhance the dissolution of water insoluble drugs such as repaglinide by a simple, non-invasive method of geometry manipulation through the use of three-dimensional printing technology that could ultimately enhance bioavailability. Additionally, the mode of treatment of repaglinide which requires continuous monitoring and adjustment makes it a perfect candidate to demonstrate 3DP abilities to create personalized dosage forms.

2.3. Three-Dimensional Printing

Three-dimensional Printing (3DP) is a method of creating 3D object by subsequent deposition of layers of materials. 3DP was first developed and used as a prototyping technique but later found application in a broad variety of fields, such as aerospace, automotive, military, sports, toys, chemical industries, infrastructure and construction, biomedical and pharmaceutical application (28). 3DP has evolved over the years from exclusively industrial tool to home fabrication and formed a huge community of 3DP enthusiasts who established a large online platform to create, share and advance 3DP.

2.3.1. Brief History on Three-dimensional Printing

The earliest account of 3DP can be traced back to the 1960s at Battelle Memorial Institute in Ohio, USA, where attempt was made to polymerize resin by intersecting two beams of different wave length. However, the first fully realized 3DP technology was developed by Charles Hull in 1984, it was called stereolithography (SLA). SLA operated by hardening liquid polymer using UV light in order to form 3D

object (29). This was followed by the development of Selective Laser Sintering (SLS) technology developed at the university of Texas which act by melting powder material using laser beam (30).

The 1990s saw the popularizing of the term 3D printing. Drop on solid (DOS) printing technology (a technology inspired by ink-jet printing) that works by solidifying powder material by jetting of liquid binder were invented at the Massachusetts Institute of Technology (31). C.S. Grump developed the Fused Deposition Modelling (FDM) printing technology which operates by depositing hot melt of thermoplastic material, he patented his technology and apparatus and founded Stratasys Inc. in 1992 (30).

At this point, three original manufacturing companies remained in the market; Stratasys, 3D systems, and EOS. The three-dimensional printing industry manufactured printers for two categories; printers producing highly complex parts, and a more cost effective, user-friendly printers aimed to be used in modelling and prototyping (29).

By the 2000s, many original patents have expired and a growing academic interest has developed to create a non-proprietary 3D printing machine that can be easily assembled through printing of its own parts (in addition to other readily available parts for purchase), and make 3D printing available for home fabrication. These 3D printers operated using open source software and hardware which allowed them to be readily accessible and modifiable.

RepRap was a project initiated in 2005 by Adrian Bowyer from the university of Bath aiming to make a self-replicating 3D printer that operate using FDM technology. Bowyer uploaded his original design online and called people to improve on it. The first printer to come out of the RepRap project was Darwin in 2007, followed by Mendel 2009. A modified and improved version of Mendel called Prusa Mendel was released in 2010. The community later moved from making printer parts files to making a complete 3D printer kit, the MakerBot printer series. MakerBot was purchased by Stratasys in 2013 (32).

Fab@home, was a similar project initiated by Cornell University, USA. The project aimed to bring 3D printing from exclusive industrial application to home fabrication, making it accessible to the ordinary public. The Fab@home printer used syringe system to extrude different types of materials (30).

The development of 3DP has drawn the attention of the biotechnology society, 3D bioprinting offered substantial advantages over the conventional 2D bioengineering approaches. 3D bioprinting harnesses the ability to implant more than one type of cells in a culture, able to produce a scaffold that closely resembles the human tissue morphologically, and can accurately and precisely deposit cells into the scaffold. These advantages are either unachievable or problematic using the traditional scaffold technology. The term 3D bioprinting expanded to engulf different applications of 3DP within the medical field, which includes human implant fabrication, customized modeling, biomimic scaffold, drug testing and control drug releasing (33).

In 2003, Mironov et. al., successfully printed the first living cells using ink-jet printer (34). This opened the gates for the tremendous advancement that 3DP can bring to tissue engineering and has been the subject of research ever since. In 2009 Organovo® released the first commercial bioprinter, and the International Society for Biofabrication (ISBF) were founded in 2010. Bioprinting has been and still experiencing substantial growth on both the academic and industrial fronts and is regarded as one of the most promising biotechnologies (35).

2.3.2. Classification of Three-dimensional Printing Technologies

Ever since 3DP first introduction to the world, numerous technologies have been developed with each carrying their own advantages and drawbacks. To understand three-dimensional printing, we classify them according to their base build material physical nature into (36):

- **Powder Solidification**
- **Liquid Solidification**
- **Extrusion Based Printing**

Powder Solidification

In this section, DOS (Drop on Solid), and SLS (Selective Laser Sintering) falls Figure 2.1. In DOS, also known as powder bed jetting, powder is turned into 3D object by the binding action of liquid binder, which is dispensed accurately on desired section of the powder material platform. The unbound powder serves as mechanical support to

the 3D object. After each successful layer fabrication, the build platform lowers and new powder is introduced for subsequent fabrication. This mechanism is the basis for ZipDose® technology developed by Aprecia® Pharmaceuticals and used to produce the first FDA approved drug SPRITAM® in 2015 (37). On the other hand, SLS operates by sintering or melting powder material using high energy beam, while build platform is lowered and new powder is introduced after every layer sintering. After successful fabrication of the 3D object the bed is slowly cooled down to produce the final print.

Liquid Solidification

Similar in concept to powder solidification, fabrication of 3D object is done through solidification of liquid material. Liquid solidification can be further classified into DOD (Drop on Drop), and SLA (Stereolithography). In DOD, liquid material is sprayed from a nozzle and cured by cooling or high energy light Figure 2.1. Due to its liquid nature, support material is needed to keep the protruded parts from collapsing. SLA uses high energy light for solidification of photosensitive polymer resins. The fabricated object is attached to the building platform which is sunk in the polymer. After solidification of a layer, the build platform descends and new layer of liquid polymer is introduced. Some SLA printers operate in an inverted plane. Here, the light source is situated below the resin tank which has a clear window bottom for the light to pass through. The tank is coated with non-sticking material and the building platform is lowered into the tank. The building platform is raised distances equal to layer thickness after each layer printing.

Extrusion Based Printing (EBP)

In extrusion-based printing, semi-solid, melt, or gel material is extruded through a nozzle onto a build platform. The printing head is raised after extrusion of each layer, ascending distance is equal to layer thickness, which is determined by the needle/ nozzle orifice diameter. The 3D object resolution is directly controlled by layer thickness which is determined by nozzle orifice diameter and printing settings.

EBP can be broadly classified into two distinctive categories:

- Fused Deposition Modelling (FDM)
- Semi-solid Extrusion Printing (SSE)

FDM operates by continuously feeding a thread (filament) of thromboplastic polymer into a screw system to be melted then extruded through a nozzle onto the building platform (bed) (Figure 2.1), in a similar fashion to hot melt extrusion (HME) process. These filaments are commercially available and can also be produce by hot melt extrusion (HME) of polymers (38). Melocchi et al. have successfully produced filaments made out of pharmaceutical grade polymers (39). However, materials to be made into filament needs to possess certain criteria.

Semi-solid Extrusion Printing (SSE) runs in a similar fashion to FDM but differs in some critical points. SSE uses semisolid, gel, melt, or liquid as a building material for its 3D objects. They are loaded into a syringe system and is extruded through a needle. SSE is heavily employed in the bioprinting industry. However, it was researched for pharmaceutical dosage form fabrication. Our 3D printer operates according to the SSE principal Figure 2.1, and the mechanism of printing is explained in more details in section 2.3.4.

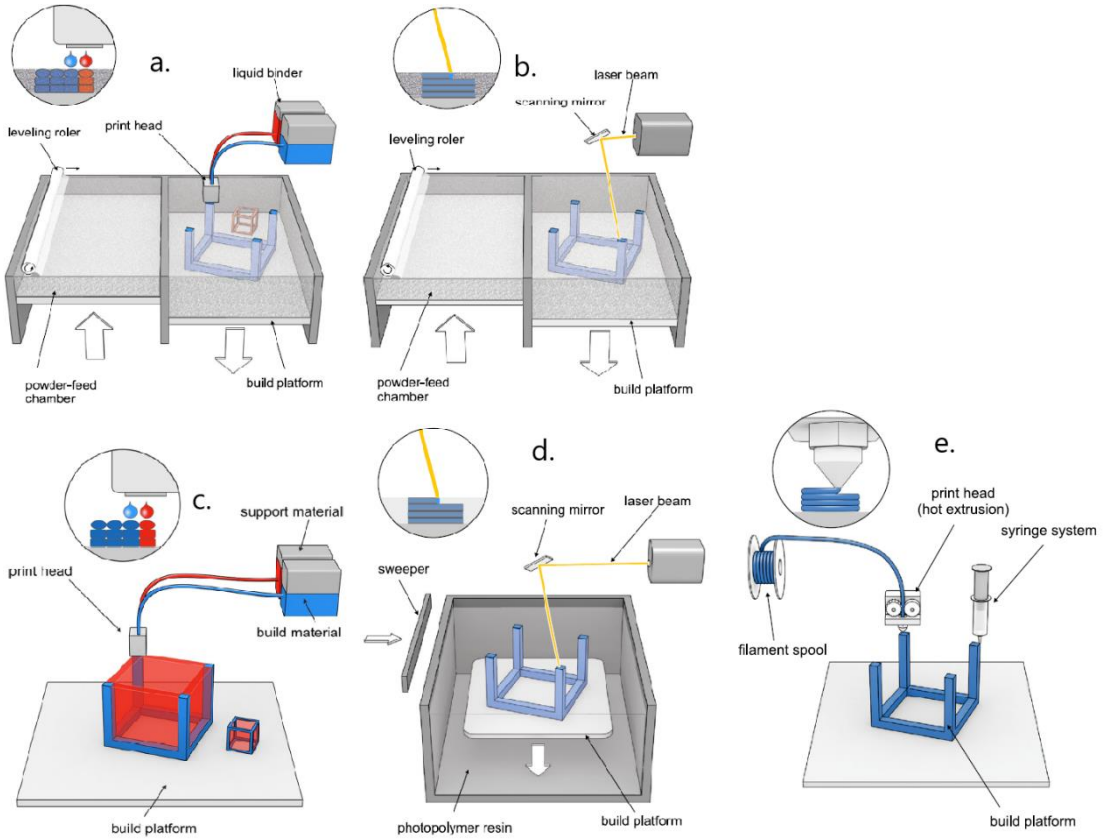

Figure 2.1. The various 3D printing technologies mechanism; (a.) DOD drop on solid, (b.) SLS Selective Laser Sintering, (c.) DOD Drop on Drop, (d.) SLA Stereolithography, (e.) Extrusion Based Printing (Filament and Syringe system) (36).

2.3.3. Applications of 3DP within the Pharmaceutical Field

3D printing had found its way within the pharmaceutical industry with the first marketed drug SPIRITAM® being approved by the FDA in 2015 (37). Researches has been conducted employing the various 3D printing technologies in producing pharmaceutical dosage forms Figure 2.2. The advantages that 3D printing provide makes it an attractive alternative to less flexible conventional production method and as previously mentioned a tool for personalized therapy.

The freedom that 3DP provides in designing and production of complex geometry had been explored in solid dosage forms to achieve diverse desired properties. Perforated tablets were successfully produced to accelerate tablet disintegration and drug release Figure 2.3 (40).

Figure 2.2. Example of pharmaceutical dosage forms developed by different 3D printing technologies from (36)

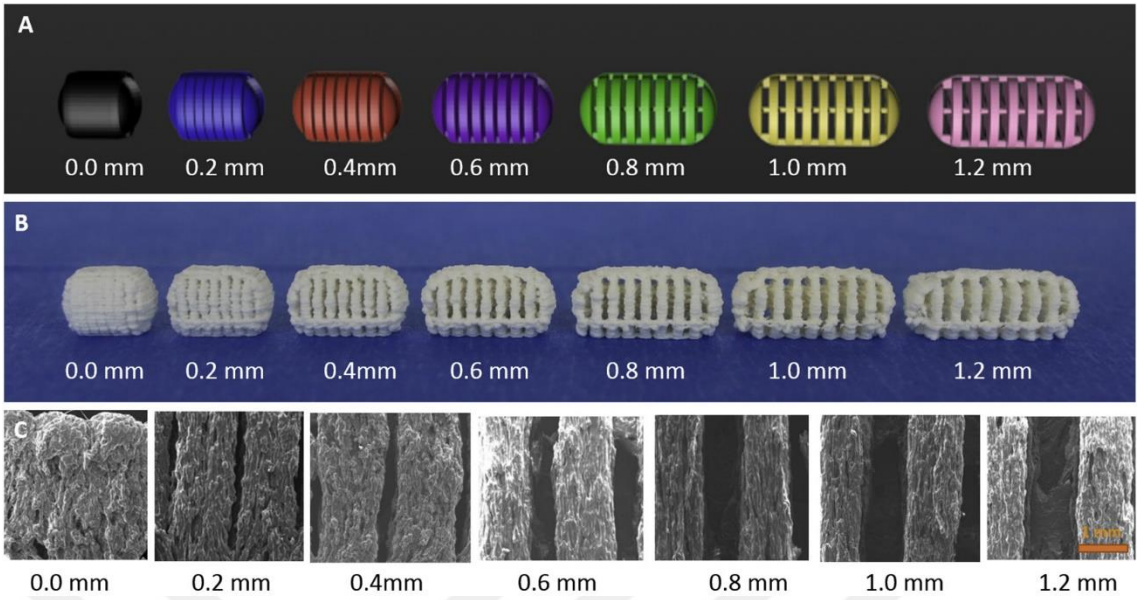

Figure 2.3. Channeled tablets to accelerate disintegration drug release from IR formulation (40).

Paracetamol tablets of different shapes were printed and the resulting tablets had different release profile Figure 2.4 (41).

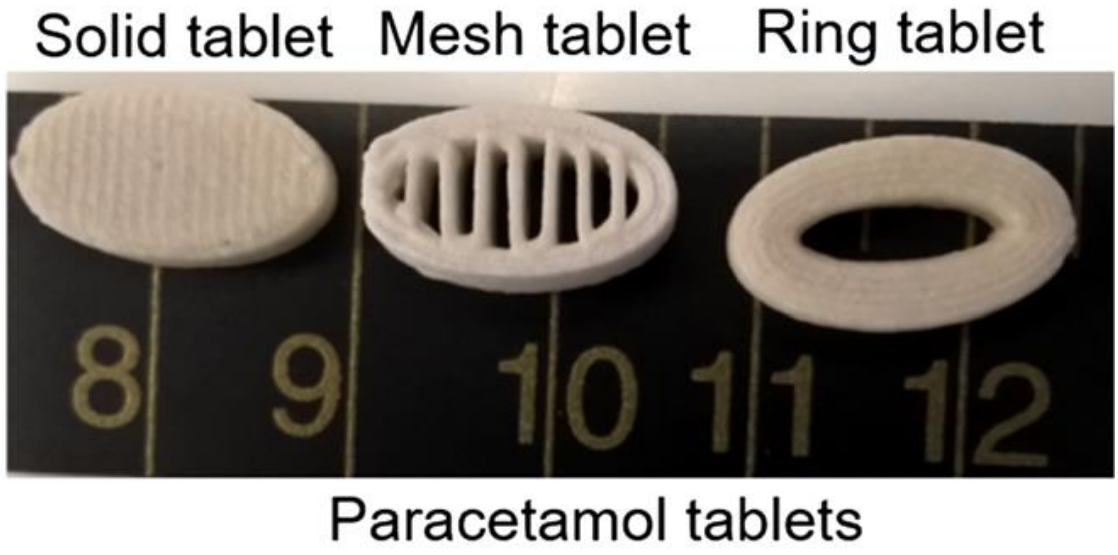

Figure 2.4. 3D printed Paracetamol tablet of different shapes with diverse release profile (41)

Tablets with varying thickness and drug load were printed, emphasizing the ability of this technology to produce tablets with desired dosage (42). Tablet surface area to volume (SA/V) impact on release behavior were investigated by Martinez et. al. (43), tablets are shown in Figure 2.5.

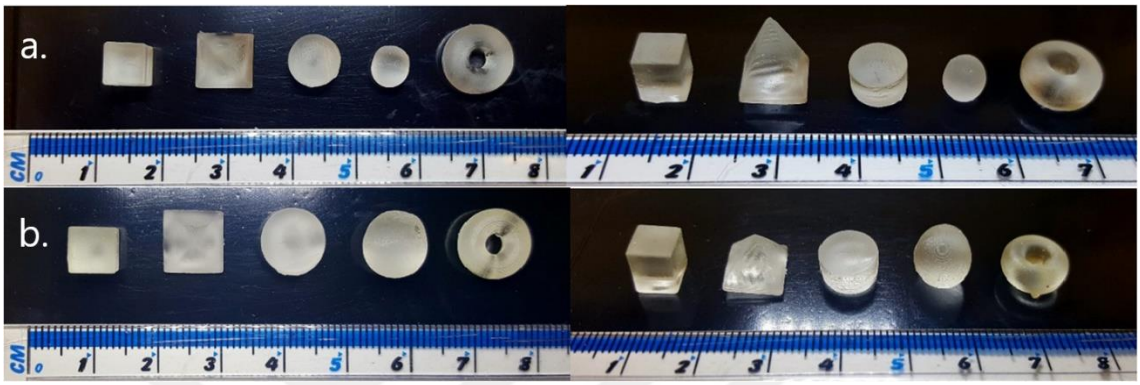

Figure 2.5. (a.) 3D tablets of similar ratio (SA/V), (b.) 3D tablets of different (SA/V) ratio; SA/V = Surface area to volume (43)

Öblom et. al. printed isoniazid tablet of varying drug load through adjustment of their size as an attempt to personalize dosing as well as release (Figure 2.6) (44).

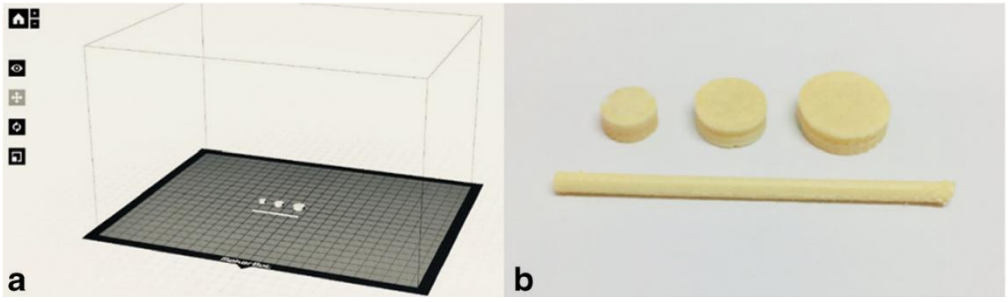

Figure 2.6. 3D printed Isoniazid tablet of varying size/dose (a) Digital model (b) tablets and filament (44).

Multi-drug treatment regimen is a major reason for treatment adherence issues. This is particularly problematic due to the fact that people who take multi-drug regimen are, in large part, patients who suffer chronic illnesses which quitting treatment or forgetting a dose could results in severe consequences. To reduce the pill-burden, tablets of complex geometry that can carry numerous drugs is a viable option. Multi-compartmental tablets (Figure 2.7) containing various drugs with diverse release profile was developed by Khaled et. al. (45-46), and Pereira et. al. (47) shown in Figure 2.8.

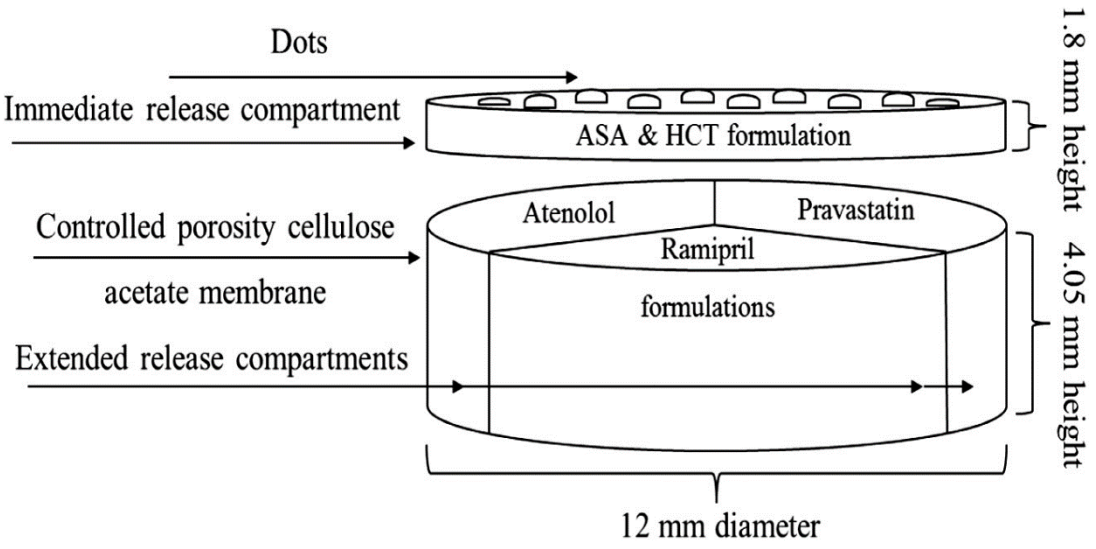

Figure 2.7. 3D printed Polypill, consisting of multiple compartments of different drugs for immediate and sustained release by Khalid et. al. (45)

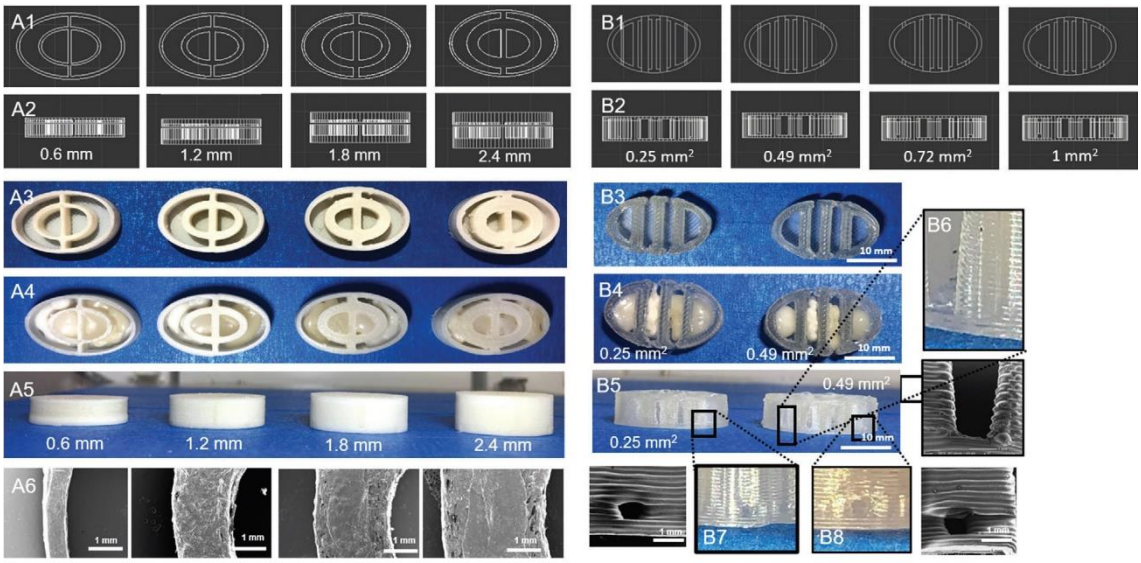

Figure 2.8. Multi-compartmental 3D printed tablet against cardiovascular diseases, containing different drugs for early and sustained release (47).

Timed release was also explored using 3DP. Pulsatile drug release was achieved through fabrication of a capsular device with varying wall thickness and composition attaining timed ruptured of capsules (48) Figure 2.9.

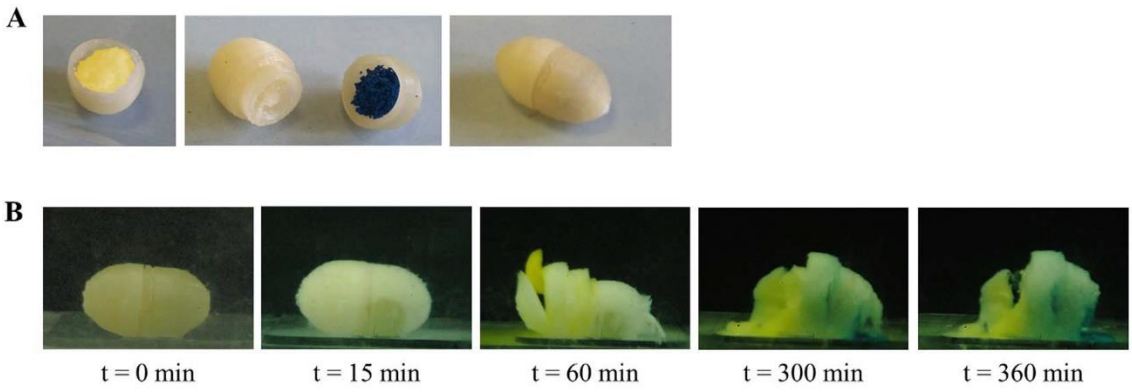

Figure 2.9. 3D printed capsular devise for timed pulsatile release (A) actual tablet (B) timed images of tablet in dissolution test (48).

The freedom to control size, dose, shape and release made possible by 3DP can be used to personalize medication and medication regimen for patients. For example, printing of smaller tablets can target pediatric patients who may normally had to break a marketed tablet in half. Designing of shape may increase acceptance or improve swallowing. Control of release can offer the freedom of singular of multiple daily dosage (18) Figure 2.10. The potential is as big as creativity can take us when it comes to personalized medication and 3DP.

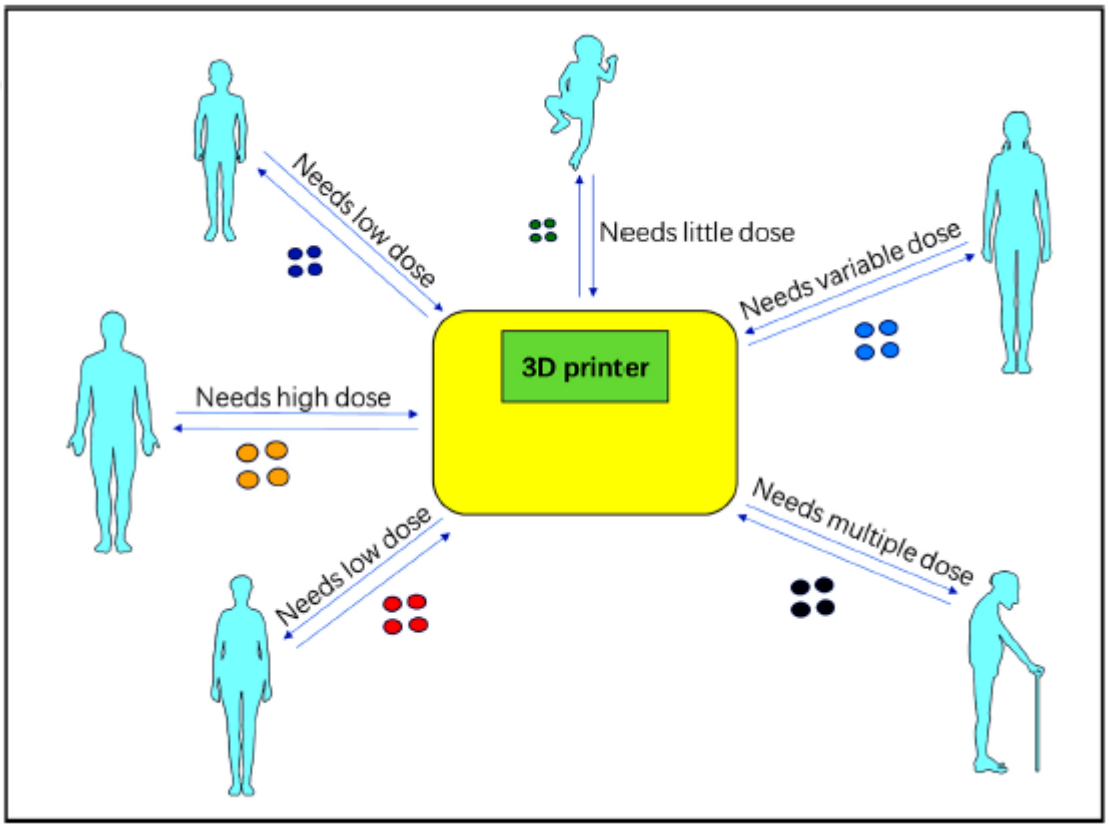

Figure 2.10. 3D role in promoting personalized therapy from (18)

2.3.4. Bioplotter and How It Works

EnvisionTEC Bioplotter is a Semi-Solid Extrusion based syringe-system bioprinter developed for biofabrication. It is employed in bone and cartilage regeneration, cellular and organ printing, soft tissue regeneration, and scaffold implants

with controlled drug release. Recently, it was used in manufacturing of tablet dosage forms (49-50).

How it operates

The printer works by dispensing melt, liquid, gel or paste from a material cartridge through a needle tip onto a stationary bed from 3-axis moving system to create a 3D object. The paste is dispensed by using air pressure provided by a compressor Figure 2.11.

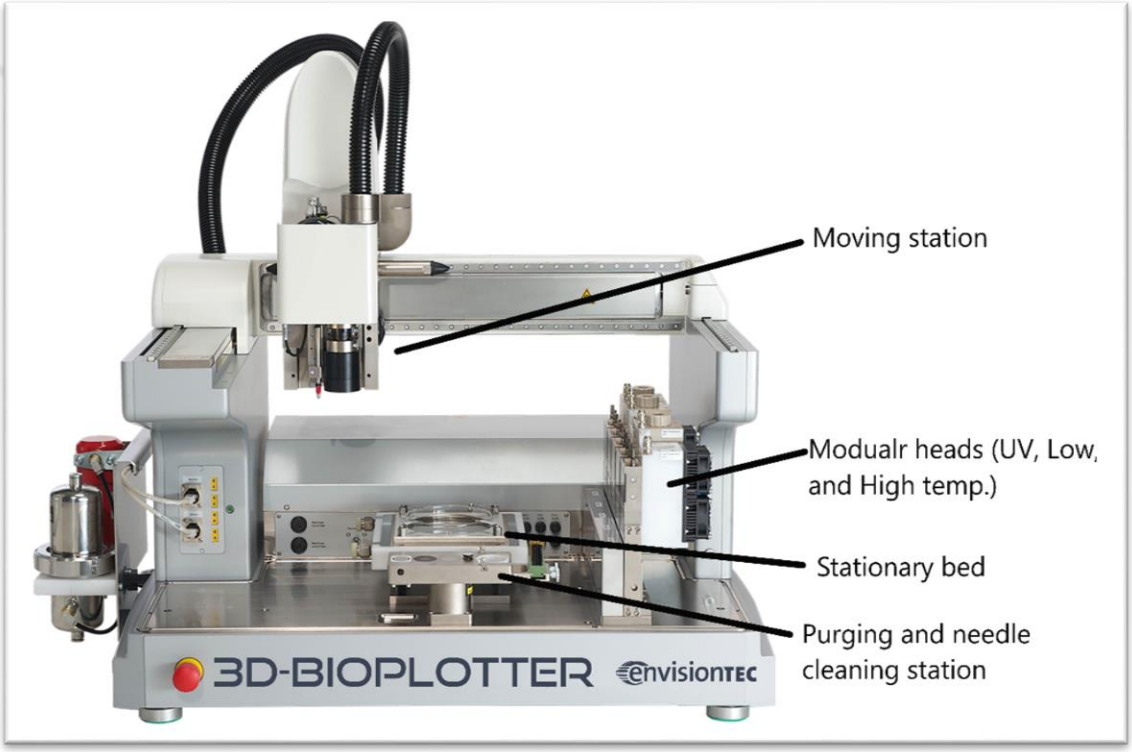

Figure 2.11. EnvisionTEC Bioplotter (Developer Series)

3DP process starts with digital design of the object. For this purpose, several Computer-Aided Design programs or CAD can be used. The design file is exported as STL file and then imported into the 3DP operating program. Settings are then applied and printing begins.

For our study, we designed our cylindrical tablets using EnvisionTEC Prefactory® RP program. We imported our design into the machine operating program (VisualMachine). Printing settings, parameters, filling pattern and strand distance among others are selected. These includes; pressure, speed of printing, offset height, transfer height, temperature, distance between each filling strand and shape of filling.

The ink (paste, gel, or melt) is loaded into a cartridge, then is fitted with a blunger and cap (Figure 2.12). A suitable needle with the desired orifice diameter is then installed, needles are generally classified according to their heat resistance and orifice diameter. Smaller needle means thinner strands/filaments which results in objects with higher definition and details. However, not all paste has the necessary physical properties to be extruded through small orifices. Furthermore, smaller orifices require using higher pressure which may cause the liquid to separate and results in blockage.

Figure 2.12. Loaded cartridges equipped with blunger and a needle

The cartridge is installed inside the modular head (Figure 2.13) and the pressure nozzle is attached. Choice of modular head is dependent on the nature of the paste; types of modular heads are shown in Figure 2.14. The moving station will attach to the modular head and move it into printing position (Figure 2.11). Pressure is applied to start extrusion and the head will move in a 3-axis plane over a stationary bed depositing layer over another in a sequence.

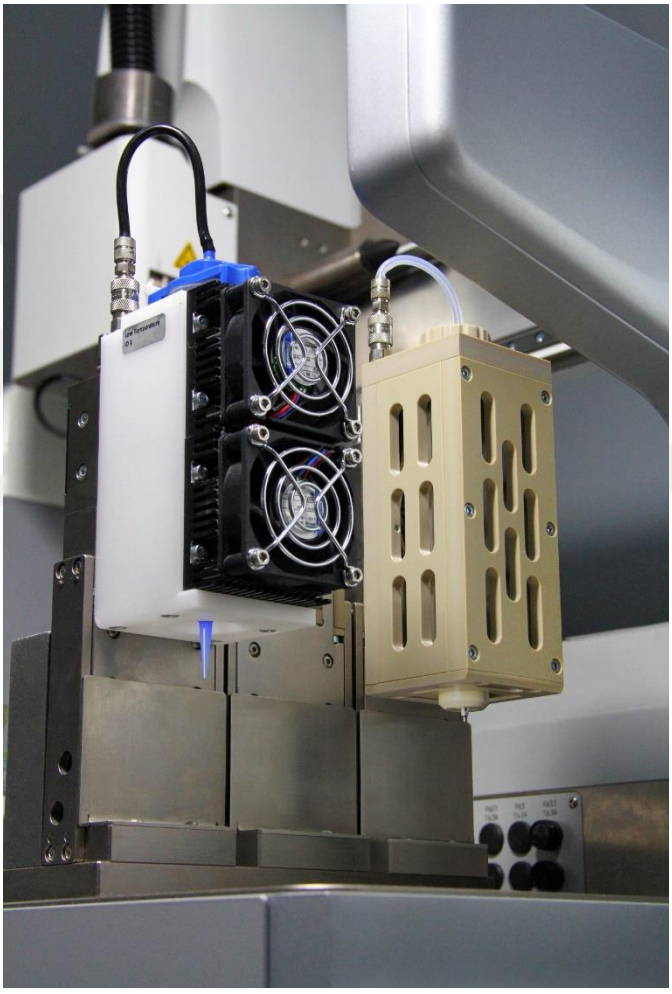

Figure 2.13. Loaded cartridge fitted inside the low temperature modular head

Head type	Temperature range	Cartridge size
Low Temperature Dispensing Head	0 - 70°C	30 ml
High Temperature Dispensing Head	30 - 250°C	10 ml
Ultra-High Temperature Dispensing Head	30 - 500°C	12 ml
2-Component Dispensing Head	25 - 70°C	50 ml
Co-Axial Low Temperature Dispensing Head	0 - 70°C	2 x 10 ml
Ink Jet Dispensing Head	25 - 70°C	10 ml
Photo-Curing Head	5 wavelength combination, user adjustable 365, 385, 395, 405, 445 nm	

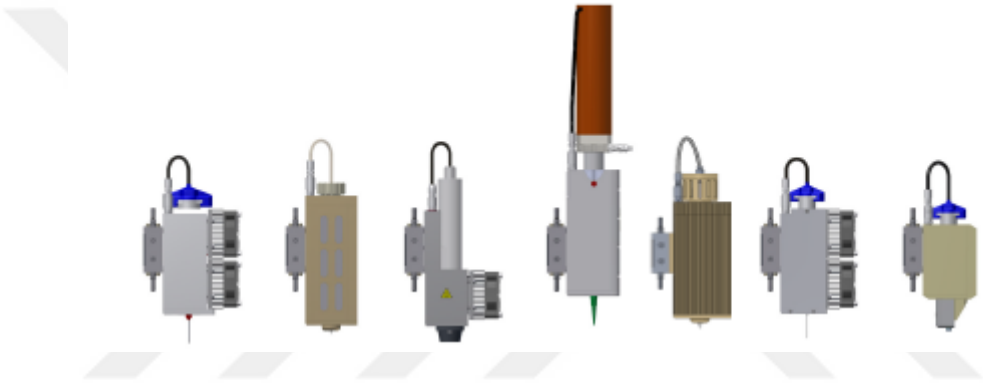

Figure 2.14. Modular heads types and specifications

Printing of 3D objects starts firstly by extruding the outer circumference/ contour of every layer. Secondly, filling of the space within the layer starts. The filling is done by extruding strands from one side of the contour to another. Pattern of the filling shown in Figure 2.15 and the distance between strands can be controlled using the operating program.

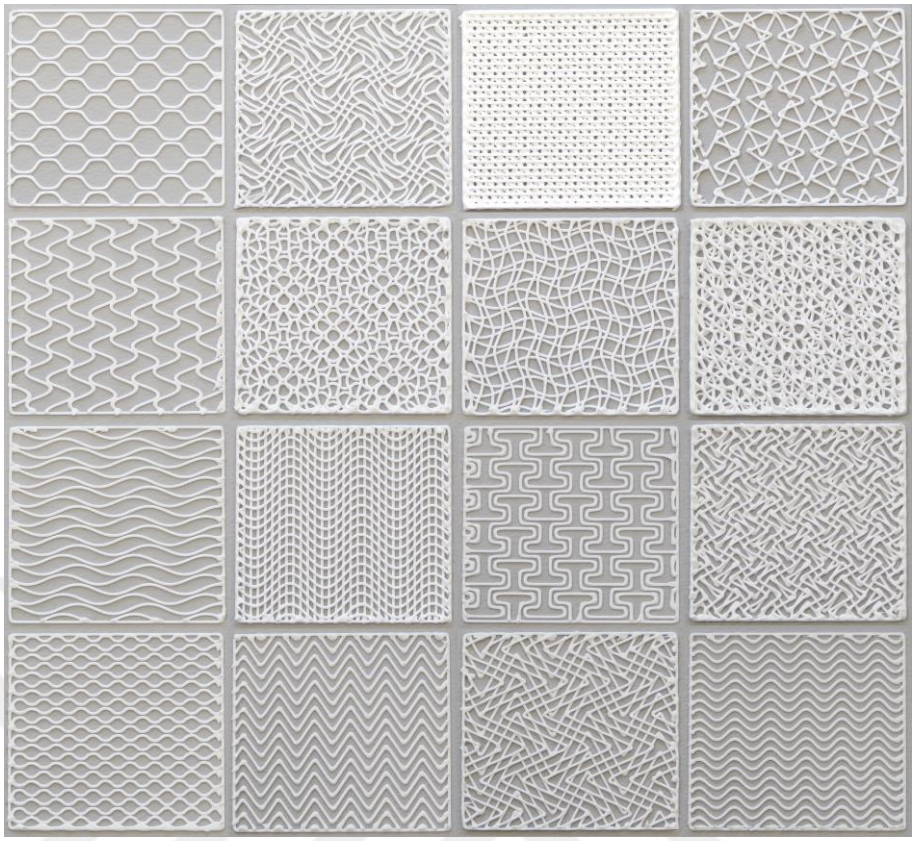

Figure 2.15. Filling patterns available for the Bioplotter (EnvisionTEC)

3. MATERIALS AND METHODS

3.1. Materials

The materials used in the study are listed in Table 3.1 along with their sources.

Table 3.1. List of materials

Materials	**Source**
Ammonium Acetate	Merck
D(+)-lactose Monohydrate	Flucka Biochemika
Disodium Hydrogen Phosphate Heptahydrate,	Analytical Grade
Glacial Acetic Acid	Analytical Grade
HPMC100K mPa.s (Methocel® 100K) substitution type 2208	Spectrum Chemical
HPMC 15K mPa.s	Aldrich Chemistry
HPMC 4k mPa.s (Methocel® E4M, Premium CR) Substitution type 2910	Spectrum Chemical
Methanol	HPLC-grade, multiple companies
Polyethylene Glycol PEG 6000	Flucka Biochemika
Repaglinide	Lot: A0389273, ACROS ORGANICS
Sodium di-hydrogen phosphate Anhydrous	Analytical Grade
Triethylamine	Merck

3.2. Equipment

The equipment used in the study are listed in Table 3.2 along with their company names.

Table 3.2. List of equipment

Equipment	**Companies**
ATR-FTIR System	Thermo Scientific Nicolet iS50 ATR/FT-IR
3D Bioprinter	Bioplotter Developer Series EnvisionTEC
Cartridge	Nordson EFD Optimum® Syringe Barrels 30 cc
Dissolution Apparatus	PharmaTest PT-DT7
Differential Scanning Calorimetry	Perkin Elmer DSC 600
Hardness Tester Apparatus	PharmaTest PTB 311E
HPLC System	Agilent 1100 Series, USA
Millipore Simplicity UltraPure Type 1 Water System	Serial no. F7CA82544, Merk
Needle/Nozzle	Nordson EFD Precision Tips Blue 0.41 mm
Reverse Phase Column	Agilent Zorbax SB-C18, PN: 883975-902
Scanning Electron Microscope	Zeiss EVO 40
Sputter coater	BAL-TEC SCD 005

3.3. Methods

3.3.1. Identification of Repaglinide using ATR-FTIR Spectroscopy/ DSC

The FTIR-ATR transmittance spectrum of pure repaglinide were obtained using Nicolet iS50 ATR/FT-IR system from Thermo Scientific and compared to the spectrum collected by Olteanu et al., 2014, to ensure authenticity of our key API. DSC test on pure repaglinide were performed by heating the sample from 30 to 350° C at a rate of 10°C per minute in a calorimeter (Perkin Elmer DSC 600) and observing the graph.

3.3.2. HPLC Analytical Method for the Quantification of Repaglinide

The HPLC method used was slightly modified from the method developed by He et al. (52). Modifications to the HPLC method was implemented in order to make it suitable for our study.

Mobile phase consisted of (80:20) methanol, and 0.01 M Ammonium acetate solution containing 0.1% Triethylamine adjusted with glacial acetic acid to pH 3.0 instead of 5.0 to attain the clearest peak of repaglinide.

Agilent Series 1100 HPLC machine were used equipped with Agilent Zorbax SB-C18 column, column temperature = 22°c, flow rate = 1 mL/ min, injection volume = 20 µL, and the detection wave length is 243 nm.

Construction of Calibration Curve

Calibration curve was prepared using 0.3, 0.5, 1, 2.5, 5, 7.5, 10 µg/mL of repaglinide in Mobile phase. These series of concentration were prepared out of three different stocks with 10 µg/mL concentration. Six replicates were tested, two sets of each stock. The calibration curve was obtained by plotting the average concentration against area.

Validation of Analytical Method for Repaglinide

The method was validated by determining the following validation characteristics: Linearity, Sensitivity, Accuracy, Precision and Specificity (53).

Linearity

The linearity of an analytical procedure is its ability (within a given range) to obtain test results, which are directly proportional to the concentration (amount) of analyte in the sample. Linearity was demonstrated using a seven-point (0.3, 0.5, 1, 2.5,

5, 7.5 and 10 µg/mL) calibration curve with 6 replicates for each point. Average peak area was plotted as a function of repaglinide concentration. Linearity was observed by calculation of a regression line by the method of least square and by visual inspection of the plot.

Sensitivity

Sensitivity of the method was determined by finding the detection and quantitation limit. The detection limit is determined by the analysis of repaglinide samples with known concentrations and by establishing the minimum level at which the repaglinide can be reliably detected. Determination of the signal-to-noise ratio was performed by comparing measured signals from samples with known low concentrations of repaglinide with those of blank samples (mobile phase). Minimum concentration at which a signal-to-noise ratio was 3:1 was accepted as detection limit. Minimum concentration at which a signal-to-noise ratio was 10:1 was accepted as quantitation limit.

Accuracy and Precision

The accuracy of an analytical procedure means the closeness of the value found and reference value. On the other hand, precision of an analytical procedure means degree of scatter among a series of measurements obtained from multiple sampling of the same homogeneous sample under the prescribed conditions. Precision may be considered at three levels: repeatability (also called intra-assay precision), intermediate precision (within-laboratories: inter- days, same or different analysts, etc.) and reproducibility (between laboratories). The precision of an analytical procedure is usually expressed as the variance, standard deviation or coefficient of variation of a series of measurements.

For assessing the intra-day and inter-day (3 consecutive days) accuracy and precision, samples of 3 known concentrations (3.5, 4.0 and 8 µg/mL) were analyzed with 6 replicates (n=6) for each of these concentrations. These concentrations were prepared from a stock solution of 10 ug/mL in mobile phase.

Specificity

Specificity is the ability to assess unequivocally the analyte in the presence of components, which may be expected to be present in the course of the analysis. Three samples: Blank sample of the dissolution medium (Phosphate buffer), sample

containing all formulation excipients with repaglinide and Sample containing the formulation excipients without repaglinide were analyzed. Chromatograms of these 3 samples were compared to see whether any changes occur on the retention time of repaglinide or enough retention is possible so that repaglinide peak is not affected by any other substances.

3.3.3. Digital Design of the Perforated Tablets

The digital design of the tablet was created as a cylinder using EnvisionTec's Prefatory® RP software. The layer height was set to 0.41 mm in line with our chosen needle orifice diameter. The choice of layer height will prompt the printing head to be lifted distance equal to layer height after finishing printing a layer. The number of layers was set to 8, while the diameter of the tablets was set to 15 mm. The inner filling pattern of the tablets were chosen to be straight strands. The distance between the center of each two adjacent strands, also known as Strand Distance (SD) were set to; 1.0, 1.3, and 1.6 mm to create 3 different perforated design tablets. The tablets will be referred to in this study as (1.0SD, 1.3SD, and 1.6SD). Figure 3.1 represent digital illustration of what the tablets were designed to be.

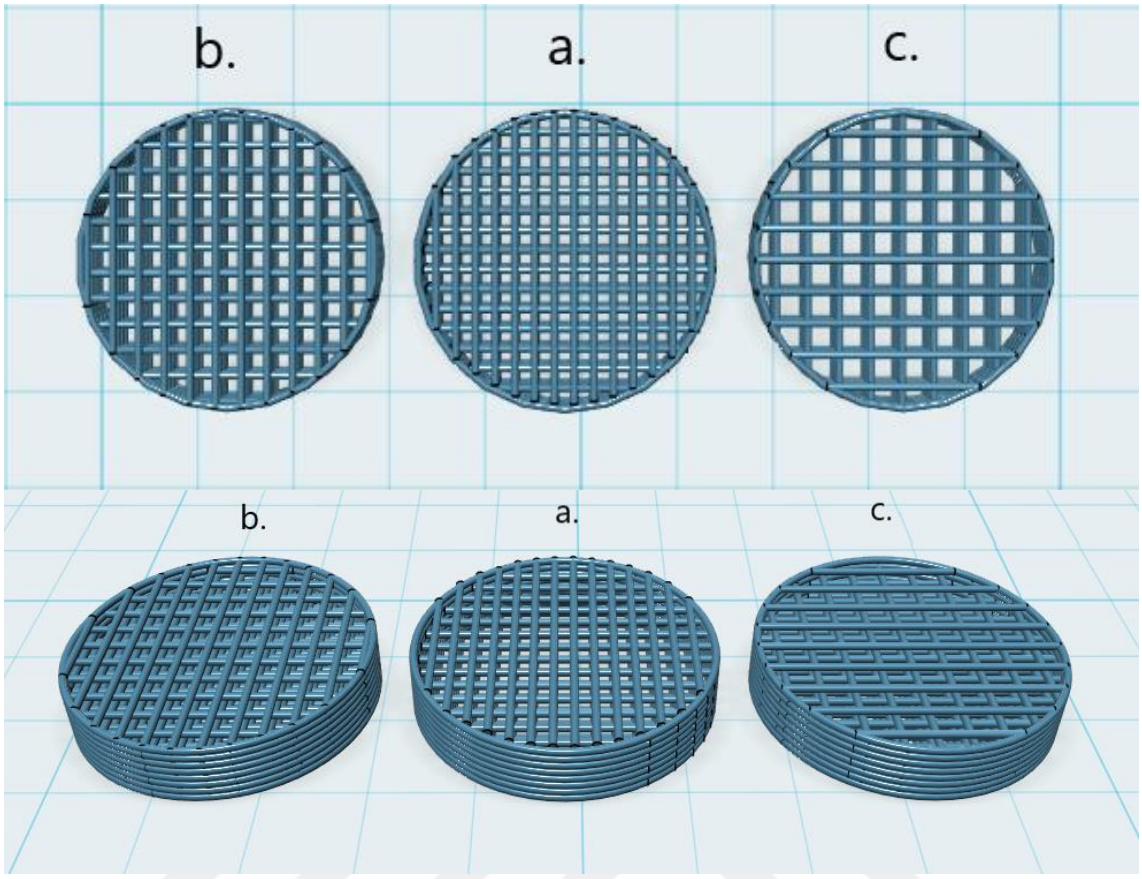

Figure 3.1. Illustration of tablet digital design (a) 1.0SD, (b.) 1.3SD, (c.) 1.6SD (SD stands for strand distance)

3.3.4. Preparation of the Binder Gel

The Binder gel prepared using the method reported in (54-55). 0.5% (HPMC E4M 2208) gel in water (w/v) were made instead of the reported 1% (w/v) HPMC 2910. 0.5 gm of HPMC E4M weighted and dispersed in 30 mL of 90° c ultrapure type 1 water. 70 gm of ice was then added and vigorously agitated for 30 minutes. the gel is then stored in fridge to release all air bubbles. Clear gel free of aggregates was formed and stored for future use (Figure 3.2).

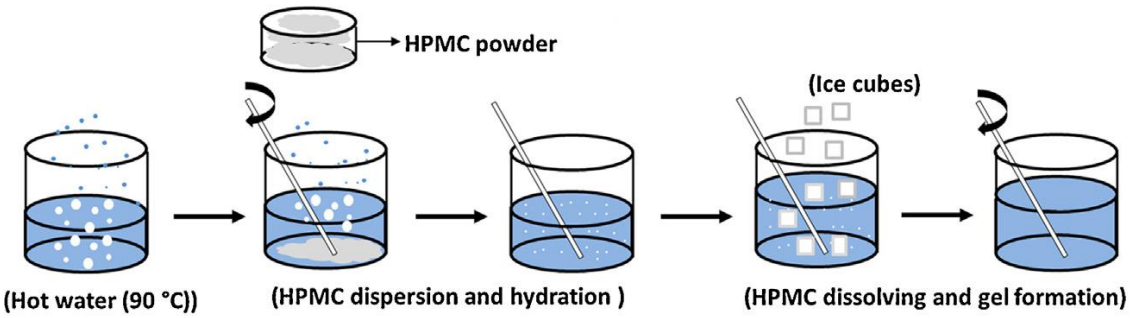

Figure 3.2. Preparation of the binder gel from (54).

3.3.5. Preparation of the Printing Ink/Paste

Mixture of the excipients powder was prepared according to Table 3.3. Polyethylene glycol (PEG 6000) crystals were grounded for 10 minutes to ensure homogenous mixture. Amount of each ingredient was accurately weighed and mixed geometrically for 18 minutes. The binder gel was then added and mixed for 10 minutes until a homogenous smooth paste was made. During and after making the paste it was kept as isolated as possible from air to avoid drying.

Preparation of Metformin paste required a different process of paste and settings optimization. Furthermore, the printing of multicompartmental design tablet demanded the use of multiple 3DP equipment and more technical experience in managing the 3D printer which unfortunately was not available for us. Hence, we decided to shift our focus into creating a singular drug tablet of various release profile.

Table 3.3. Composition of the printing ink/paste

Excipient	Function	HPMC100K Form.	HPMC 15K Form.
Repaglinide	API	20 mg	20 mg
HPMC100K,	Polymer	250 mg	-
HPMC 15K	Polymer	-	250 mg
Lactose	Filler	18750 mg	18750 mg
PEG 6000	Plasticizer	375 mg	375 mg
HPMC E4M hydro gel	Paste former/ Binder	1.8 mL	1.6 mL

3.3.6. Semi-solid Extrusion Printing of Tablets

The printing process started by carefully loading the paste into the printing cartridge using a spatula avoiding air exposure as much as possible. A blunger is then placed inside to help extrude the paste evenly and preventing it from retreating upward when printing. Next, the cartridge cap was shut. a suitable needle with 0.41 mm orifice width was installed. The printing cartridge is inserted inside the low temperature modular head, which was equipped into the moving printing station (Figure 2.11) (further information in 2.3.4. section).

The following printing settings were used; Pressure = 4 bars, speed = 2 and 3 mm/s for 15K and 100K formulation respectively. Temperature was not employed in our experiments and was set in accordance with laboratory temperature (22 ± 2°c). 8 layers were deposited for each tablet. After printing, the tablets were left in room temperature for a day to dry up.

It is worth noting that loading process is performed as quickly as possible to avoid drying. Furthermore, uniform loading and distribution of the paste inside the cartridge was ensured during this process. To ensure extrusion of continuous strands, small amount of the ink is purged before printing starts.

When printing starts, the printer extrudes the outer circumference/contour of the tablet first, then filling starts by extruding of strands extending from one side of the contour to the opposite side.

The distance between the center of each two adjacent strands can be adjusted and is set to 1.0, 1.3, and 1.6 mm to create 3 tablets of different strand filling of each formulation (100K, and 15K). After the deposition of one layer is complete, the deposition of the next one starts. The angle of deposition of one layer atop of the other can be adjusted and is set to 90° resulting in a cage like structure (Figure 3.1).

3.3.7. Evaluation of the Printed Tablets

The mechanical strength of a tablet which expressed as hardness and friability reflects its resistance to breakage, chipping and attrition that is associated with the different steps of production, packaging, and shipping. The smaller scale, more personalized clinical setting that our tablets are intended for, exposes them to far less strenuous conditions. Nevertheless, hardness and friability studies were conducted on

small group of specimens to assess their mechanical strength. Test of tablets size over multiple samples were conducted to assess shape consistency over various prints. Size was assessed through measurement of tablet thickness and diameter.

Hardness and Size

Hardness, thickness and diameter of tablets were tested using Pharma Test PTB 311E apparatus. 18 tablets were tested, 3 different tablets of each geometry of the two formulations. Approximate nominal information of thickness, width and hardness were entered into the digital screen of the apparatus. Millimeter (mm) and kilopond (Kp) selected as units. Each tablet was placed upright onto the driven jaw and the test begun. The jaw will run forward till the tablets is touched to measure the thickness, thereafter it reverses back and the tablet falls into horizontal position to measure diameter and hardness. When touched, the machine gradually raises force until breakage occurs. The 3 results are then displayed on screen and the test is repeated.

Friability

Friability of tablets was tested using Pharma Test PTF-ER friability testing instrument. 18 tablets, 3 tablets of each different geometry of the two different formulations. the tablets were cleaned thoroughly with a brush and their weight is carefully recorded. The tablets were then loaded into the apparatus and it ran for 100 revolutions. The tablets were taken out, brushed carefully to remove any excess powder and their weight accurately recorded. The differences in weight were calculated as percentage of original total weight.

Drug content

Out of each formulation, 12 tablets were weighed and crushed. Amount of powder equivalent to the average weight of one tablet (260 mg, 290 mg) for HPMC 100K and 15K formulation respectively, weighed separately and dispersed in 100 mL of methanol and stirred for one hour (46). The sample is then filtered using 0.42 µm filtered and drug content is determined using HPLC machine.

Scanning Electron Microscopy (SEM)

The tablets cross and horizontal section were sputter coated with Au-18k using ion sputter mc 1000. The tablets were examined under Zeiss EVO 40 scanning electron microscope. The tablets were observed from the top and were sliced by a cutter to have

a cross sectional view in order to investigate their geometrical integrity and surface morphology.

In vitro Drug Release

Dissolution study was carried out using basket apparatus 1, PharmaTest PT-DT7 dissolution apparatus. Dissolution medium was phosphate buffer pH =6.8, 0.1 M prepared using (Disodium hydrogen phosphate heptahydrate, and sodium di-hydrogen phosphate anhydrous). Dissolution parameters were as follow; Rotation speed of baskets = 50 rpm, temperature = 37 °C ± 0.5°C, dissolution volume = 900. The test was conducted for 12 hours. Samples were taken at t=15 minutes to ensure no burst release took place, then were taken at t=1 hour and at every 2 hours interval. 6 tablets were tested at one time and the test was repeated 3 times (n = 3). Sample volume was 5 mL and was replaced with same amount of fresh medium each time. The samples were then filtered through a 0.42 µm filter and injected into the HPLC machine for analysis using automatic injector.

3.3.8. Comparison of Dissolution Profiles

Similarity (f_2) and Difference (f_1) Factors

In order to objectively evaluate the similarity or difference between pairs of different tablets, the model-independent mathematical method developed by Moore and Flanner (56) was used. The factor f_2, called the similarity factor, measures the closeness between the two dissolution profiles by the following equation:

$$f_2 = 50 \log \left\{ \left[1 + \frac{1}{n} \sum_{n-1}^{n} (R_t - T_t)^2 \right]^{-0.5} * 100 \right\}$$

The f_1 factor, called dissimilarity or difference factor, measures the closeness between dissolution profiles by the following equation:

$$f_1 = \left\{ \left[\sum_{t=1}^{n} |R_t - T_t| \right] / \left[\sum_{t=1}^{n} R_t \right] \right\} \times 100$$

where n is the number of time points, R_t and T_t are the dissolution values of the two profiles being compared at time t. All the 7 sampling time points, 1, 2, 4, 6, 8, 10, 12 h were included. In pairing the profiles, first, tablets were chosen from within the same formulation but different SD values; then, from between formulations with the same SD values; and finally, from the graphically close profiles. A value of f_2 between 50-100 shows similarity between two dissolution profiles whereas a value below 50 show dis-similarity. As the FDA and EMA have also established a public standard for f_2 value between 50 and 100 for similarity, we used this criterion for evaluating the sameness of any two dissolution profiles (57). When the value of f_1 is zero, the pairs are identical and this increases proportionally with the dissimilarity between the two profiles (57). Generally, f_1 value of 0-15 are accepted as sameness or equivalence of the two curves.

Dissolution Efficiency

The dissolution efficiency (DE) was calculated by the method originally proposed by Khan et al. (58). The related equation is:

$$\mathrm{DE} = \frac{\int_{t_1}^{t_2} y.\,dt}{y_{100}(t_2 - t_1)} \times 100$$

where t_1 and t_2 are the two time points, numerator is the integration of % release (y axis), that is, the area under the dissolution curve, the denominator is the rectangle area representing 100% release by t_2. The areas under the dissolution curve were calculated by trapezoidal rule.

During calculation, it also occurred to us that even without consideration of DE, simply comparison of individual dissolution AUCs of one tablet to another can also produce meaningful data. Therefore, such comparison was also performed.

Two-Way Analysis of Variance (ANOVA)

A two-way (formulation and strand distance) analysis of variance (ANOVA) with replication was done with a significant difference at $p < 0.05$. The initial 1, 2, and 4

hour dissolution data were analyzed where dissolution curves are apparently close to each other. The calculation was done with Analysis ToolPak of Microsoft Excel.

3.3.9. Modelling of the Drug Release Kinetics

The overall release of repaglinide from the different 3D printed tablets were evaluated by Korsmeyers-Peppas model which is commonly used for tablets where release is governed by multiple release mechanism, it is considered comprehensive, but still very simple model (59). The correlation factors were first determined between the drug release and time. On the basis of correlation coefficient, further evaluation was performed to determine the n-exponent values. The korsmeyer-Peppas model is shown below:

$$\frac{M_t}{M_\infty} = Kt^n$$

where, M_t and M_∞ are absolute amount of drug released at time t and amount of drug that was present in the tablet, k is constant incorporating the structural and geometrical modification on the dosage form, and n is the release exponent which indicates the mechanism of drug release.

3.3.10. Assessment of Drug-Excipient Interaction

Interactions of repaglinide with excipients was assessed with differential scanning calorimetry. Tablets with and without repaglinide were heated from 30 to 350° C at a rate of 10°C per minute in a calorimeter (Perkin Elmer, DSC 600). The thermograms were compared.

4. RESULTS

4.1. Identification of Repaglinide using ATR-FTIR/ DSC

ATR-FTIR spectrum, obtained by the method described in section 3.3.1, is presented in Figure 4.1 along with the spectrum reported by Olteanu et al. (51).

The DSC thermogram is presented in Figure 4.2. The start of melting range complied with the PubChem reported melting point of repaglinide.

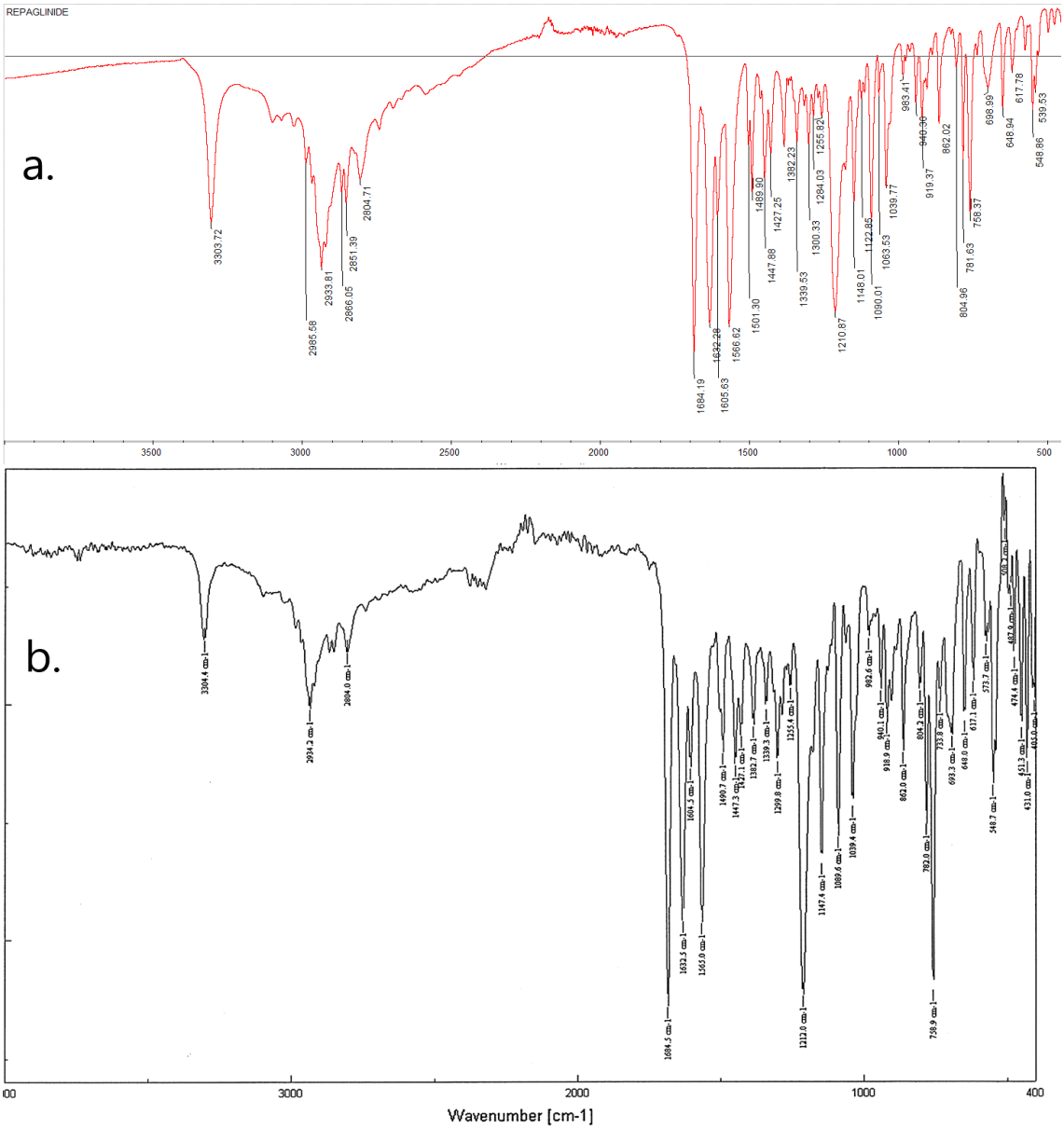

Figure 4.1. ATR-FTIR spectrum of repaglinide (a) obtained from our API using our machine (b) obtained from literature by Olteanu et al (51).

The differential scanning calorimetry (DSC) thermogram for repaglinide is shown below. The melting range was 130-138^0 C.

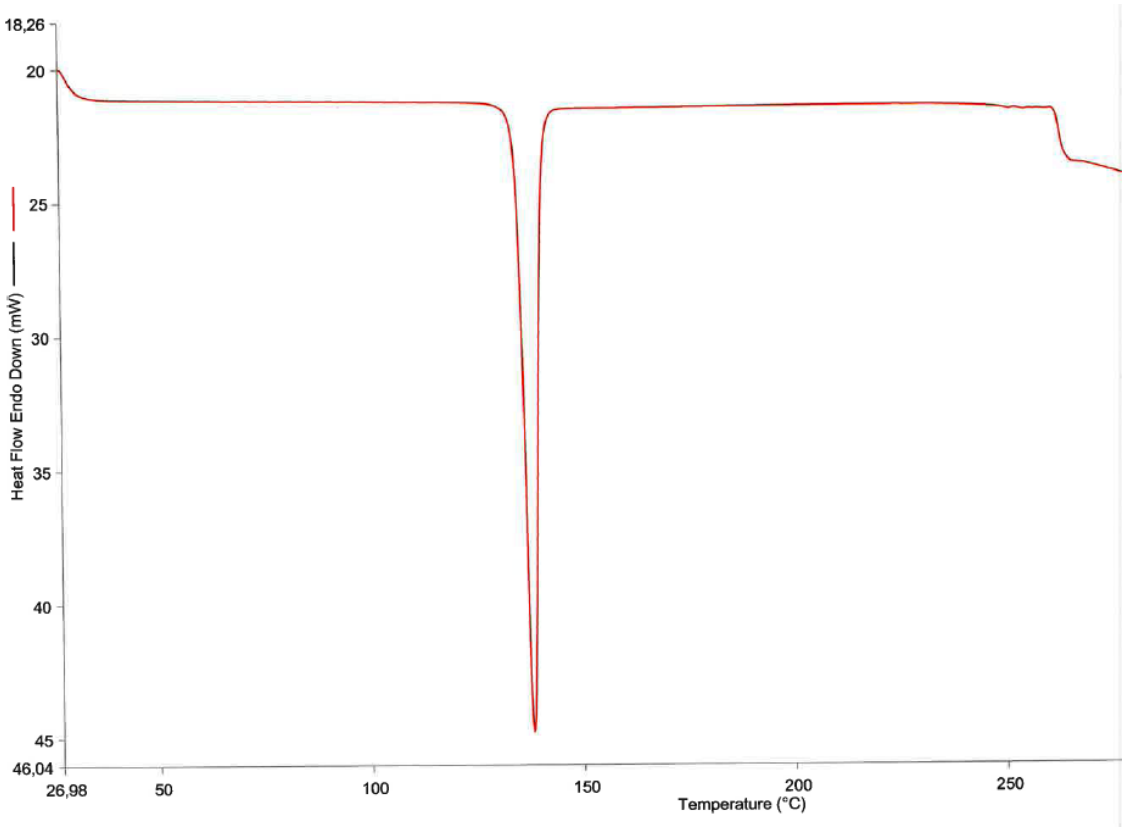

Figure 4.2. Differential scanning calorimetry thermogram for repaglinide

4.2. Quantitative Determination of Repaglinide by HPLC

Quantitative determination of repaglinide was performed under the conditions described in section 3.3.2. Figure 4.3 is a representation of the HPLC chromatogram of repaglinide in mobile phase at a concentration of (2.5 µg/mL)

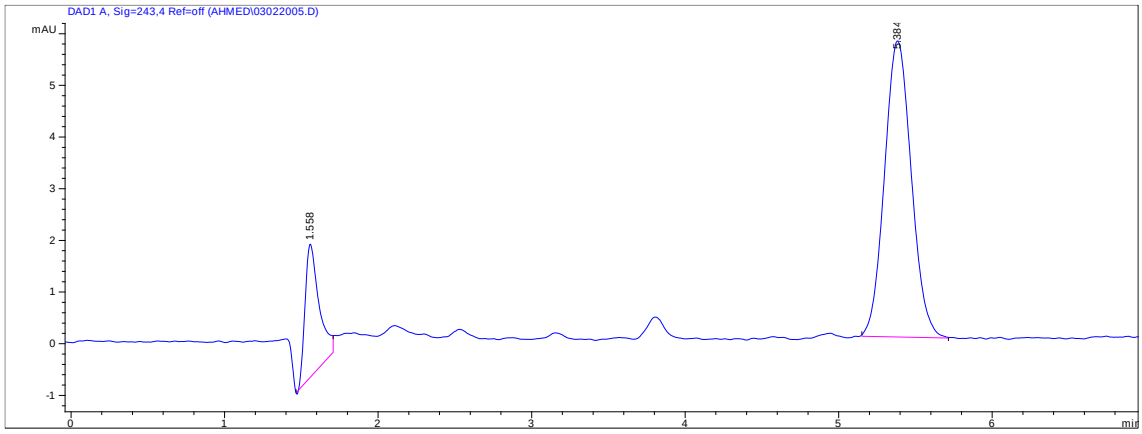

Figure 4.3. HPLC chromatogram of repaglinide in mobile phase (2.5µg/mL)

4.2.1. Repaglinide Calibration Curve

Repaglinide calibration curve was constructed according to the method described in section 3.3.2. The calibration curve is given in Figure 4.4. The slopes of the 6 replicates were calculated and had a coefficient of variation of 5.66. The analytical data of the graph is calculated as 95% confidence level (P = 0.05), reported alongside standard error at 95% confidence interval calculated using the equation below. Linear regression data for the calibration curve are reported in Table 4.1 below.

$$\boldsymbol{Standard\ Error\ at\ 95\%\ conf.} = \mathbf{2} * \frac{\boldsymbol{STD}}{\sqrt{\boldsymbol{n}}}$$

Table 4.1. Linear regression data (n=6) obtained in HPLC analysis of repaglinide

Parameter	Results
Concentration Range	0.3 µg/mL - 10 µg/mL
Slope	32.444 ± 1.499 (95% confidence interval)
Intercept	0.119 ± 0.582 (95% confidence interval)
Correlation Coefficient	0.999
Detection Limit	0.018 µg/mL
Quantification Limit	0.06 µg/mL

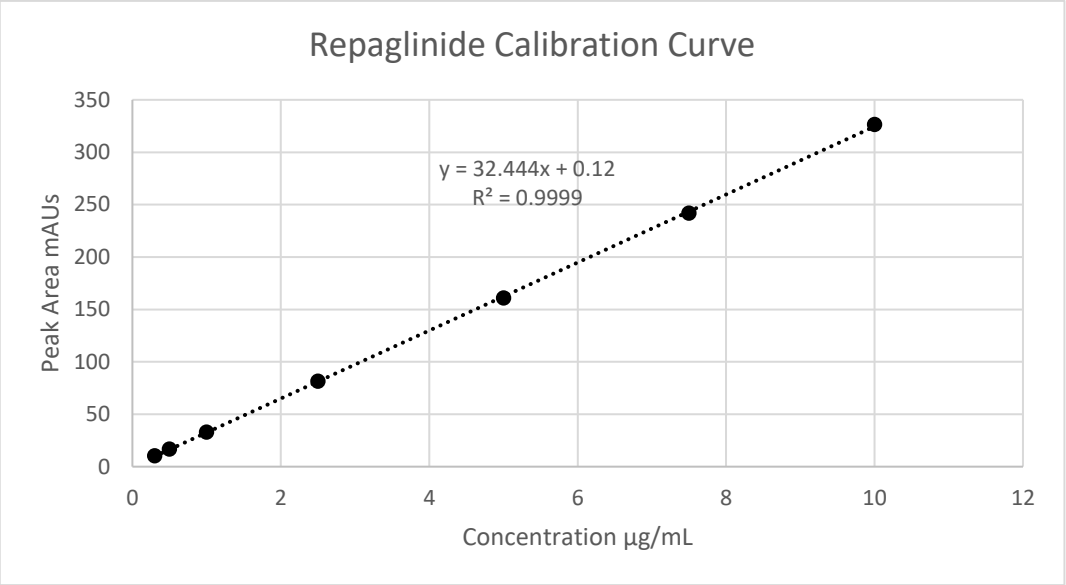

Figure 4.4. Calibration curve of repaglinide in mobile phase and regression equation

4.2.2. Validation of Analytical Method for Repaglinide

Linearity and Sensitivity

Visual inspection of the repaglinide concentration vs peak area plot clearly shows a linear curve over the range of 0.3 - 10 µg/mL. Regression analysis and correlation coefficient (0.999) also proves the linearity. As described in section 3.3.2, detection limit (signal-to-noise ratio was 3:1) and quantitation limit (signal-to-noise ratio was 10:1) of repaglinide were found to be 0.018 and 0.06 µg/mL, respectively.

Accuracy and Precision

As described in section 3.3.2., three standard concentrations (3.5, 4.0, and 8 µg/mL) of repaglinide on the calibration curve were prepared and analyzed with 6 replicates (n = 6). Assessment of intra-day and inter-day (3 consecutive days) accuracy and precision for each of these three concentrations were done. Data provided in Table 4.2, and Figure 4.5.

Table 4.2. Intra-day and inter-day accuracy and precision

	Added Concentration (µg/mL)	Found Concentration (µg/mL)	Accuracy (%)	Precision (Coeff. of variation, %)
Intra-day	8.00	7.77	2.82	0.02
	0.40	0.38	4.44	1.25
	3.50	3.39	3.02	0.07
Inter-day	8.00	7.98	0.00	1.85
	0.40	0.40	0.01	5.73
	3.50	3.48	0.01	1.92

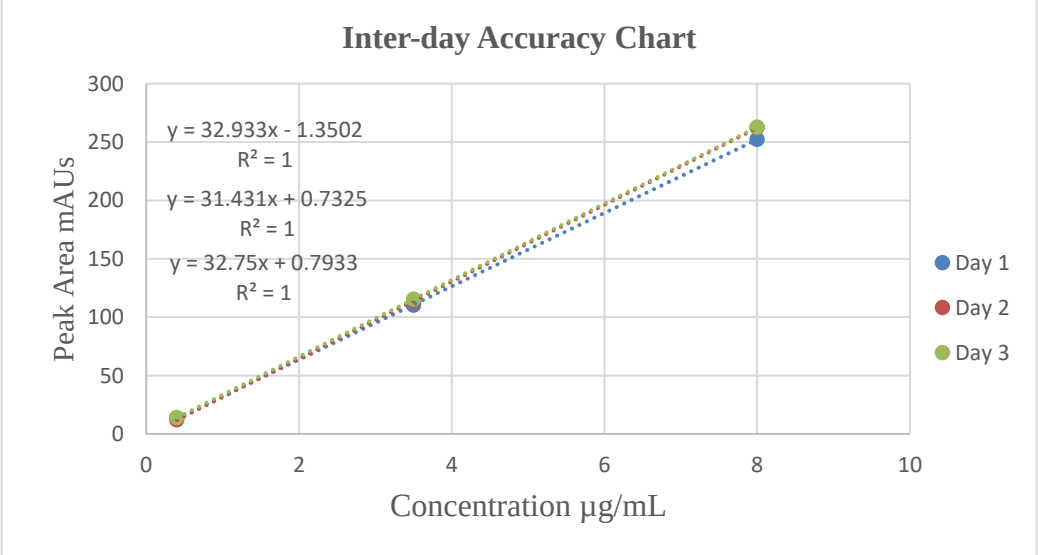

Figure 4.5. Inter-day accuracy lines (n=3) three consecutive days

Specificity

Specificity of the analytical method was proved by the method described in section 3.3.2. There was no interference to the repaglinide peak by other formulation components. HPLC graph of drug-free formulation and drug loaded one are represented in Figure 4.6.

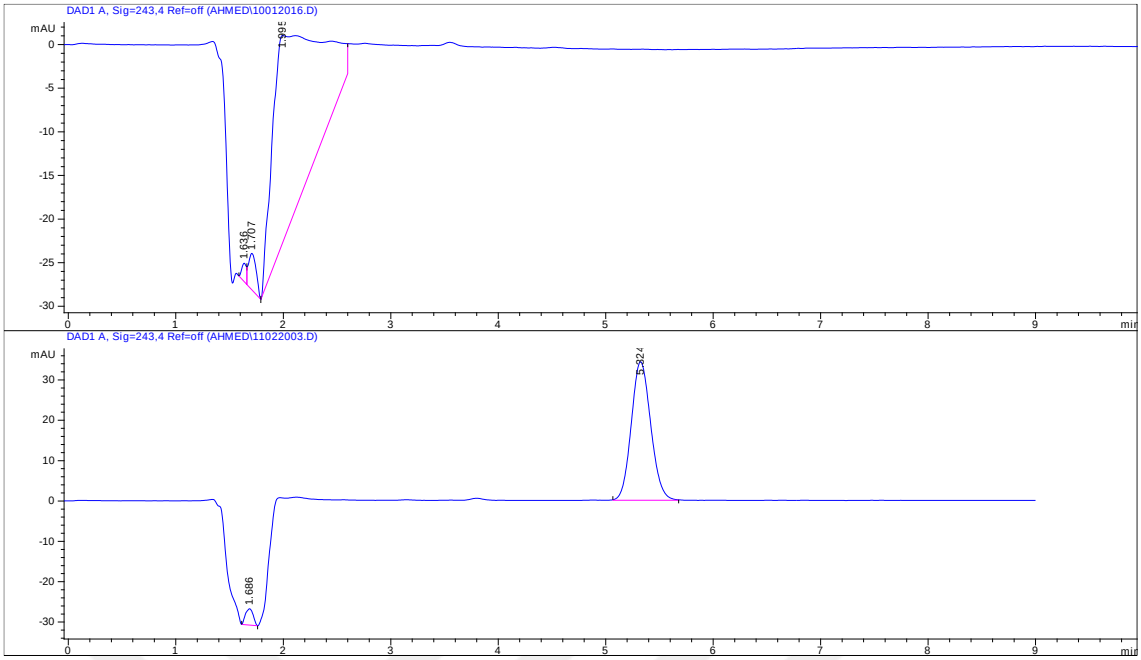

Figure 4.6. HPLC graph of Drug-free formulation (top), and Drug-loaded (bottom)

4.3. Three-dimensional Printed Tablets

One batch of the printing ink/paste produced 6 tablets ± 1. The tablets were left to dry overnight and the resulting tablets had an average 3.24, 15.13 mm thickness and diameter, respectively. The tablets had a porous, cage like structure as intended and can be easily distinguished by their pore size difference Figure 4.7-4.8.

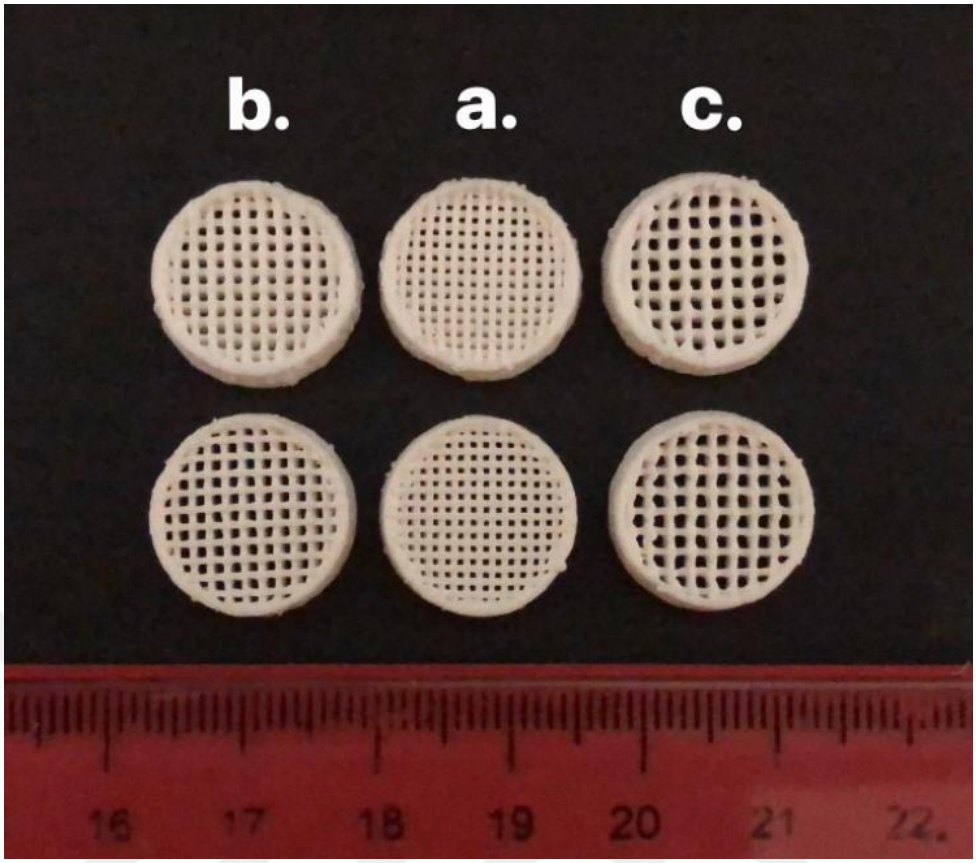

Figure 4.7. Top View of the tablets, Top 3 tablets are made with HPMC 100K, while the bottom ones are HPMC 15K formulation (a) 1.0SD (b) 1.3SD (c) 1.6SD

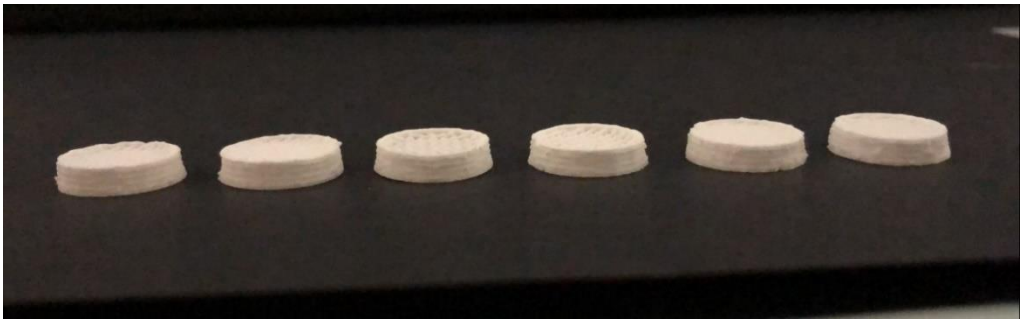

Figure 4.8. Horizontal view of the 3D printed tablets

4.4. Evaluation of the Printed Tablets

4.4.1. Size and Hardness

As described in section 3.3.7., hardness and size were assessed in 3 replicates (n = 3) of each tablet. It is worth noting that these tablets were taken out of different batches. Diameter and thickness results are reported in Table 4.3 and as box plot in Figure 4.9-4.10. Hardness results are reported in Table 4.4 and Figure 4.11.

Table 4.3. Size values of the tablets (Thickness and Diameter)

	Formulations					
	100k			**15K**		
	1.0SD	**1.3SD**	**1.6SD**	**1.0SD**	**1.3SD**	**1.6SD**
Thickness (mm)	3.31	3.23	3.23	3.23	3.24	3.16
	3.23	3.23	3.11	3.43	3.31	3.15
	3.25	3.22	3.12	3.32	3.39	3.12
Diameter (mm)	15	14.99	15.02	15.04	15.74	14.96
	15.29	14.83	15.21	15.34	15.57	14.77
	14.99	15.07	15.06	15.53	15.12	14.73

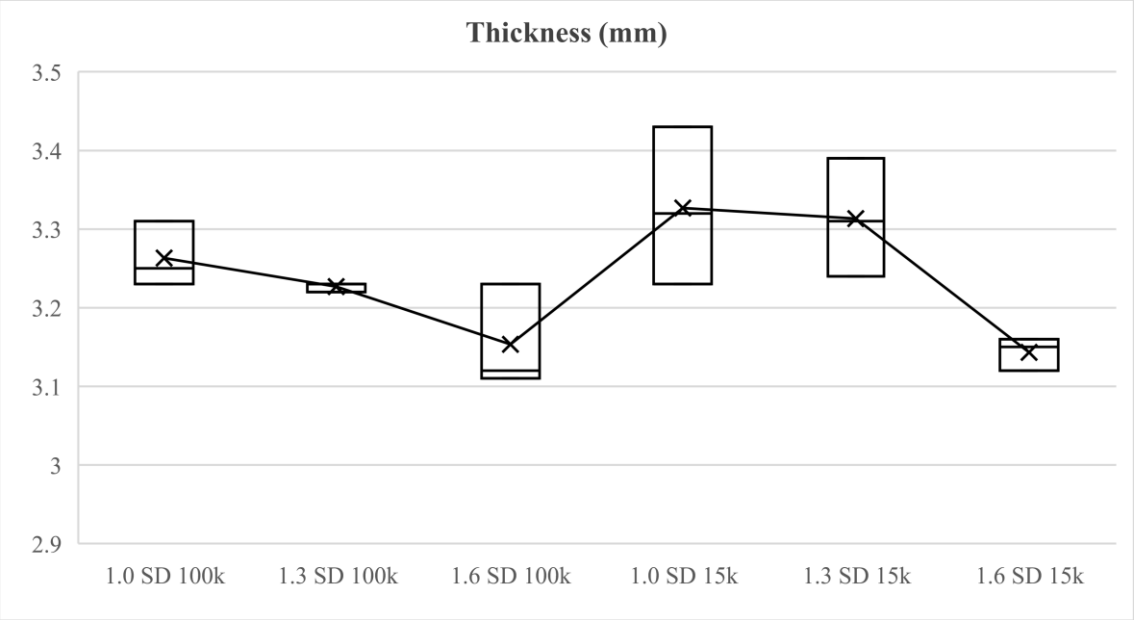

Figure 4.9. Box plot summary of tablet thickness (mm)

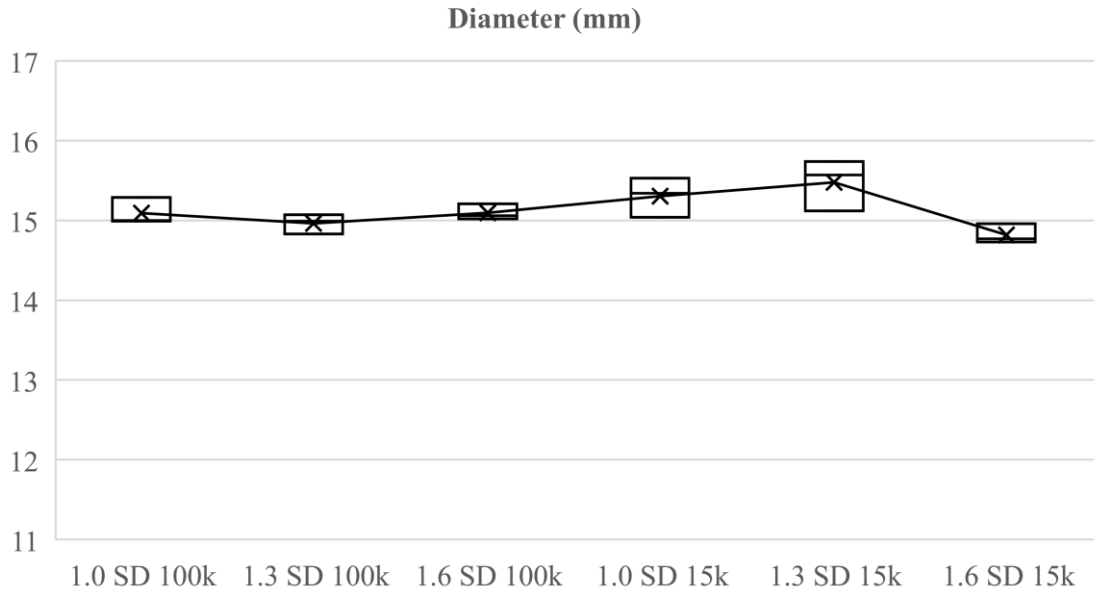

Figure 4.10. Box plot summary of tablet Diameter (mm)

Table 4.4. Hardness values of tablets in Kilopond (Kp)

	Formulation					
	100k			**15K**		
	1.0SD	**1.3SD**	**1.6SD**	**1.0SD**	**1.3SD**	**1.6SD**
Hardness (Kp)	3.5	1.2	1.2	1.6	3.4	1.1
	3.4	1.4	0.9	5.2	2.8	1.2
	2.1	1.6	0.9	4.6	1.5	0.6

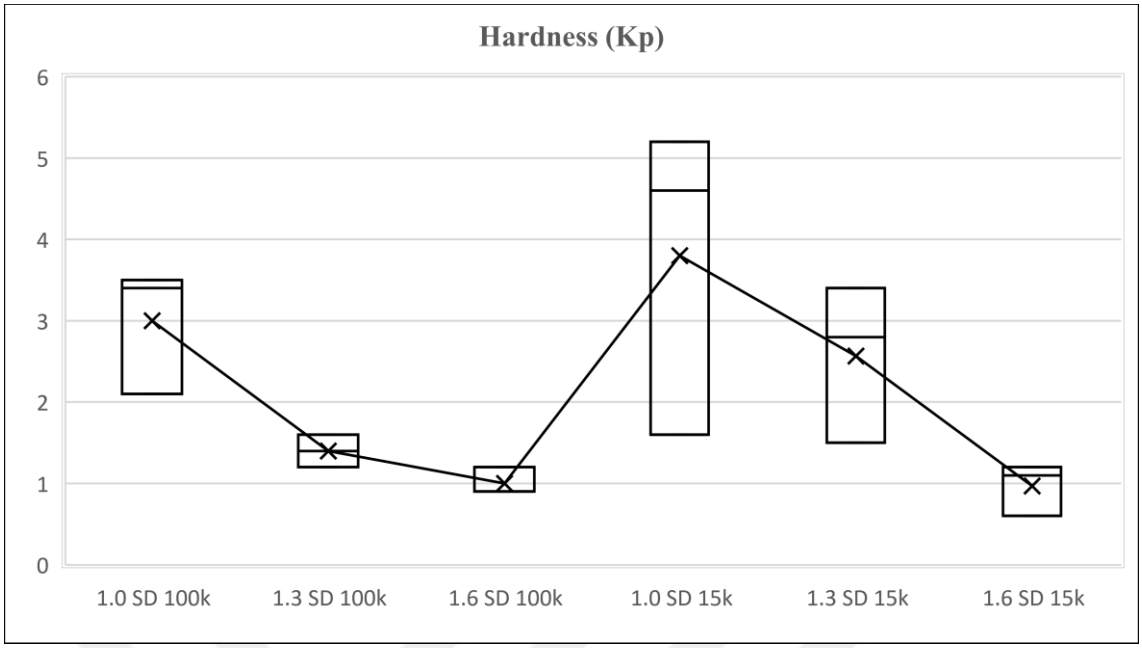

Figure 4.11. Box plot summary of hardness values

4.4.2. Weight Variation

The weight of the tablets is reported in Table 4.5 below and is represented as a box plot graph in Figure 4.12.

Table 4.5. Weight values of the tablets

	Formulations					
	100K			**15K**		
	1.0SD	**1.3SD**	**1.6SD**	**1.0SD**	**1.3SD**	**1.6SD**
Weight (mg)	312.2	228.9	251.2	273.9	331.5	190
	332	254.7	219.7	406.5	336.4	191.7
	276	260.4	223.3	411	309.1	190

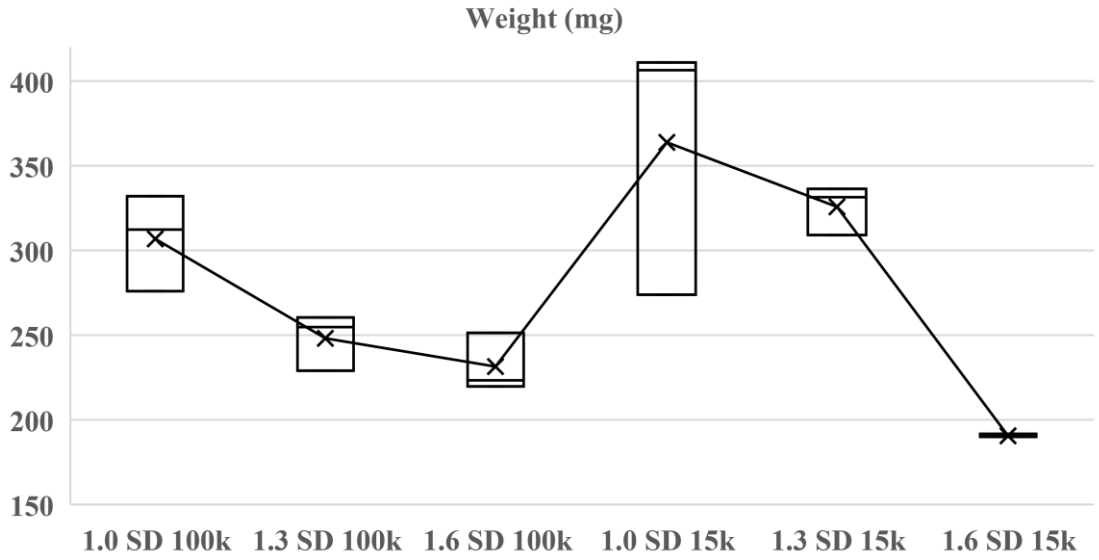

Figure 4.12. Box plot summary of weight values (mg)

4.4.3. Friability

As described previously in section 3.3.7, friability was evaluated in 3 replicates of each of the six tablets and the results are reported in Table 4.6 and represented in Figure 4.13 as percentage of the lost weight to the original weight.

Table 4.6. Friability results of the tablets

	Formulations					
	100k			**15K**		
	1.0SD	**1.3SD**	**1.6SD**	**1.0SD**	**1.3SD**	**1.6SD**
Friability, %	0.76	1.09	0.54	0.83	0.71	0.72
	0.63	0.57	0.95	1.11	0.84	0.89
	0.77	0.63	1.27	0.74	0.61	0.80

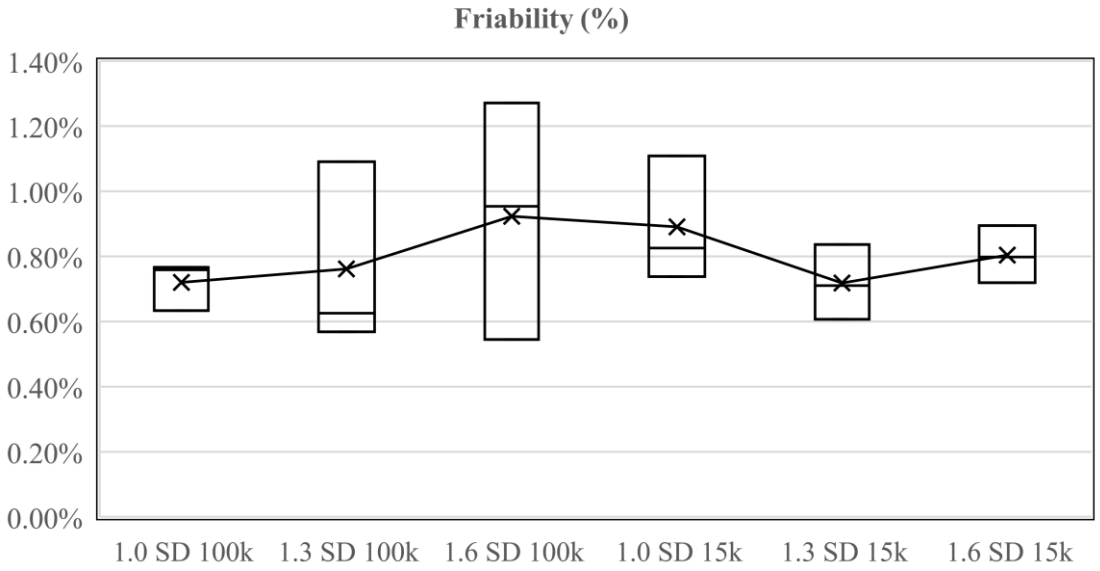

Figure 4.13. Box plot summary of Friability values

4.4.4. Drug Content

As reported in section 3.3.7, drug content test was performed on 12 tablets of each formulation. Results are reported in Table 4.7.

Table 4.7. Drug Content values for 10 samples of each formulation.

Drug Content					
15k Form.	T1	87.17	**100k Form.**	T1	95.64
	T2	90.25		T2	94.44
	T3	91.87		T3	94.42
	T4	88.91		T4	93.91
	T5	88.37		T5	90.87
	T6	92.03		T6	88.49
	T7	89.55		T7	89.79
	T8	89.22		T8	91.63
	T9	89.59		T9	89.98
	T10	91.27		T10	89.63
	Avg.	89.82		**Avg.**	91.88
	Std.	1.48		**Std.**	2.38

4.4.5. Scanning Electron Microscopy (SEM)

Results of the SEM is shown in Figure 4.14. Top and cross-sectional images were taken at 100X magnification.

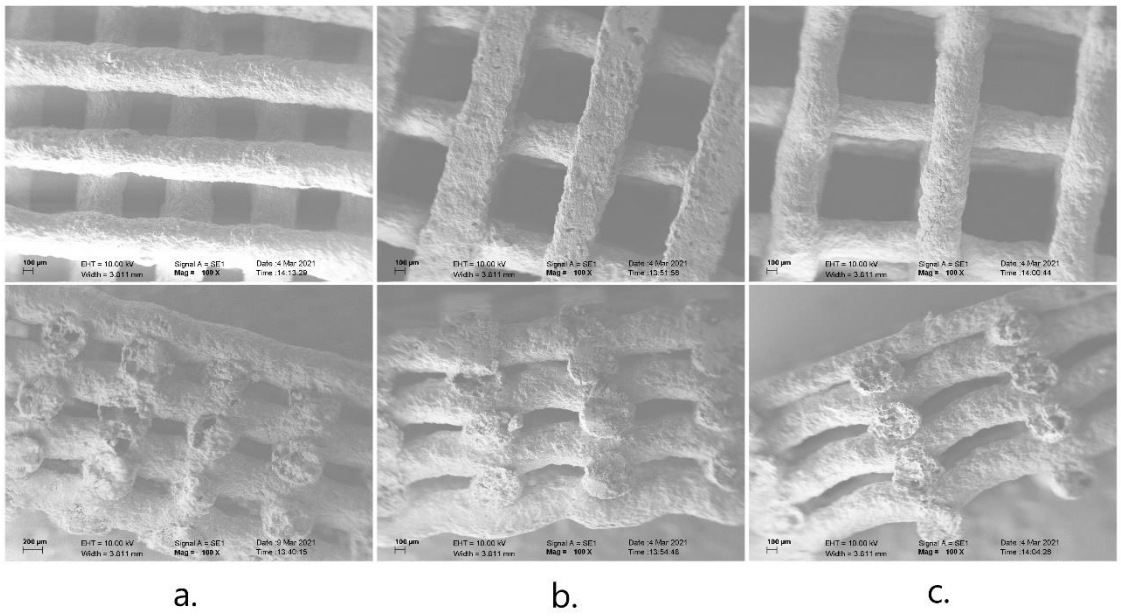

Figure 4.14. SEM images of the 3D printed tablets; (a) 1.0SD, (b) 1.3SD, (c) 1.6SD; top images are taken from over-the-top angle while the bottom images are cross-sectional.

4.4.6. Dissolution Study

As described in section 3.3.7, dissolution study was carried out on 3 replicates (n = 3) of the 6 tablets to investigate their release behavior over 12 hours period. Figure 4.15 represents dissolution profiles of the 100K formulation tablets, while Figure 4.16 shows 15K formulation. Figure 4.17 represents all the six tablets dissolution profiles superimposed in one place.

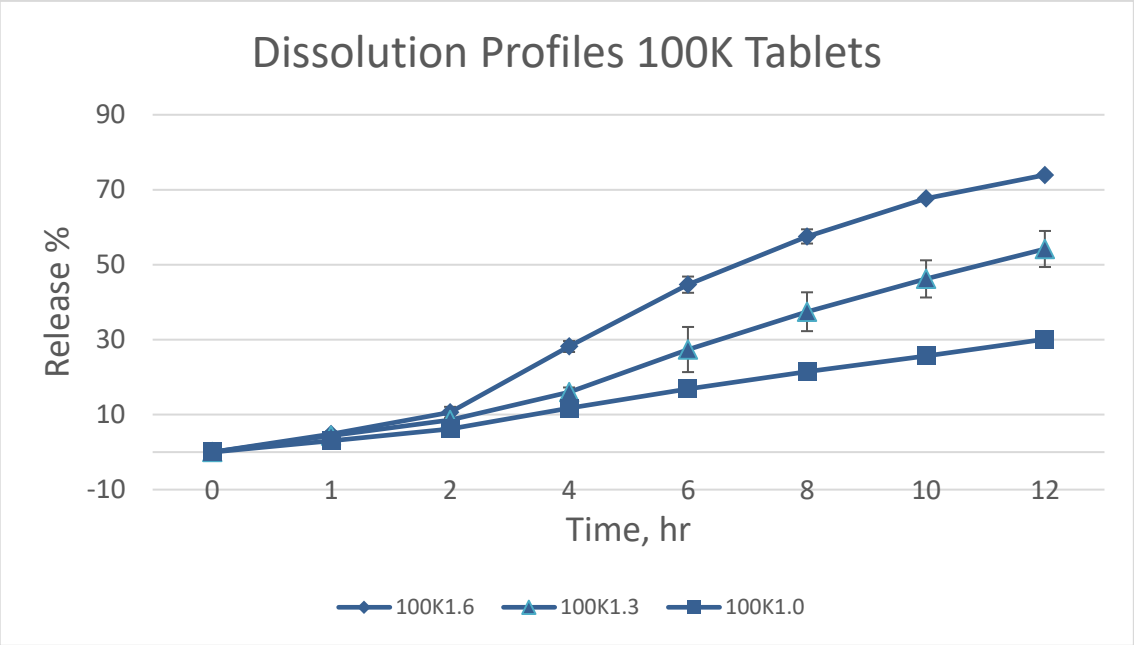

Figure. 4.15. Release profile of 100K formulation tablets (n=3) ± SD

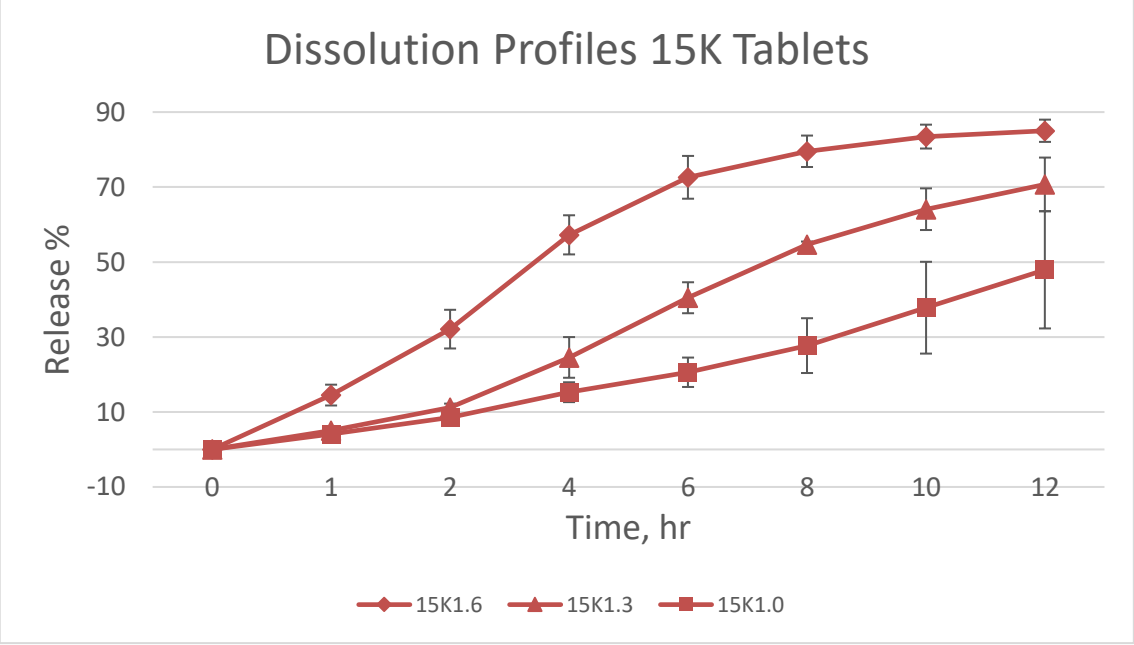

Figure 4.16. Release profile of 15K formulation tablets (n=3) ± SD

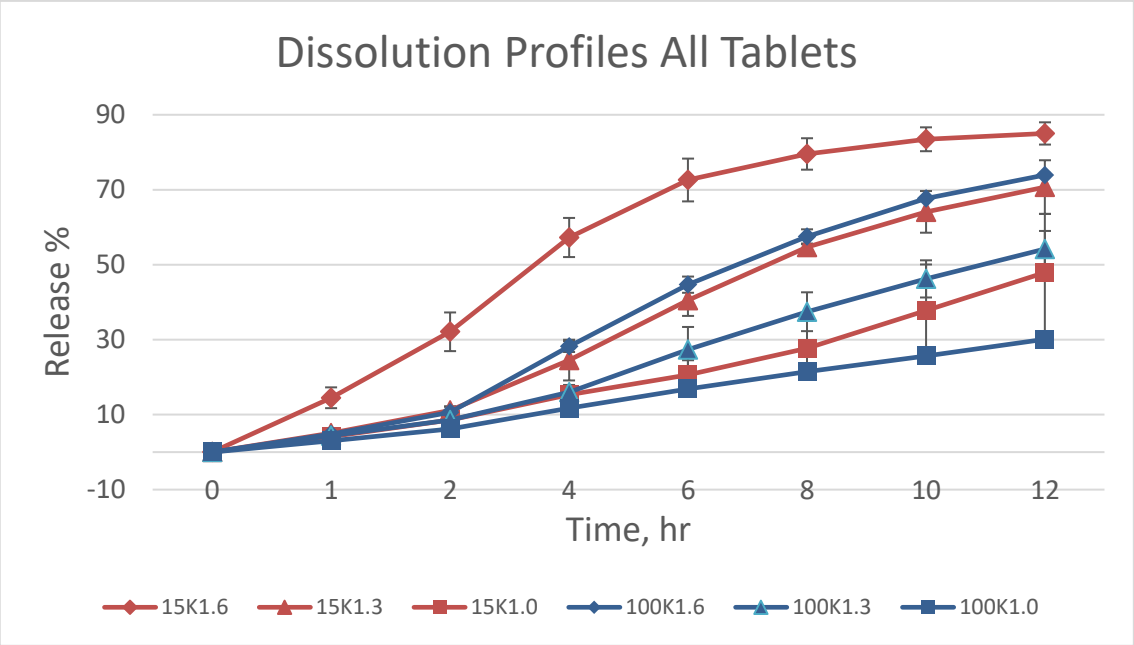

Figure 4.17. Release profiles of the 6 tablets (n=3) ± SD

4.4.7. Comparison of Dissolution Profiles

The results of the comparison by the similarity and difference factors are reported in Table 4.8 below.

Table 4.8. Similarity (f_2) and difference factor (f_1) values for different pairs of tablets

Pairs		**f_2**	**f_1**
(1) Between 15K Tablets			
15K1.6	15K1.3	31.53	36.24
15K1.6	15K1.0	19.81	61.85
15K1.3	15K1.0	36.47	40.17
(2) Between100K Tablets			
100K1.6	100K1.3	40.29	32.45
100K1.6	100K1.0	26.57	59.96
100K1.3	100K1.0	42.47	40.72
(3) Between Same SD Tablets			
15K1.6	100K1.6	34.04	32.30
15K1.3	100K1.3	44.63	28.28
15K1.0	100K1.0	**52.74**	28.93
(4) Graphically Close-by Pairs			
15K1.3	100K1.6	**75.10**	**6.74**
15K1.0	100K1.3	**60.81**	19.89

The results of dissolution efficiency calculations and comparison of AUCs within formulations (different SDs) and in relation to highest area provider (15K1.6SD) are presented in Table 4.9.

Table 4.9. Dissolution efficiency (%), AUCs (%-h) and comparison of AUCs

Tablets	**DE, 12 h**	**AUC(0-12h)**	**Within Formulations**		**Relative to 15K1.6**
100K1.0	16.16	193.96	39.52		26.45
100K1.3	27.12	325.43	66.31	Relative to 100K1.6	44.37
100K1.6	40.89	490.74	100.00		66.91
15K1.0	22.30	267.59	36.48		36.48
15K1.3	38.34	460.03	62.72	Relative to 15K1.6	62.72
15K1.6	61.12	**733.42**	100.00		100.00

4.4.8. Modelling of Drug Release Kinetics

The Korsmeyer-Peppas model associated correlation coefficient and n-exponent of values in addition to the predicted release mechanism are shown in Table 4.10 below.

Table 4.10. Korsmeyer-Peppas model fit data and the predicted release mechanism

Tablets	**n**	**r^2**	**Release Mechanism**
100k 1.0SD	0.868784	0.999722	Anomalous
100k 1.3SD	1.036809	0.998984	Super Case II
100 k 1.6SD	1.119421	0.99802	Super Case II
15K 1.0SD	1.083407	0.996517	Super Case II
15K 1.3SD	1.143053	0.999777	Super Case II
15K 1.6SD	0.92	0.998545	Super Case II

4.4.9. Two-Way Analysis of Variance ANOVA

The results of analysis are shown in Table 4.11.

Table 4.11. Two-Way ANOVA results of perforation and formulation

	1h		2h		4h	
	F	P-value	F	P-value	F	P-value
Among SD	39.45	$5.3X10^{-06}$	61.09	$5.1X10^{-07}$	124.50	$9.4 x10^{-09}$
Formulation	41.10	$3.3X10^{-05}$	63.64	$3.9 X10^{-06}$	75.23	$1.6 X10^{-06}$
Interaction	24.42	$5.9 X10^{-05}$	32.96	$1.3 X10^{-05}$	24.43	$5.9 X10^{-05}$

4.4.10. Assessment of Drug-Excipient Compatibility

The differential scanning calorimetry thermograms are presented in the following Figures 4.18 and 4.19 as a comparison between drug-free and drug-loaded formulation for 15K and 100K, respectively.

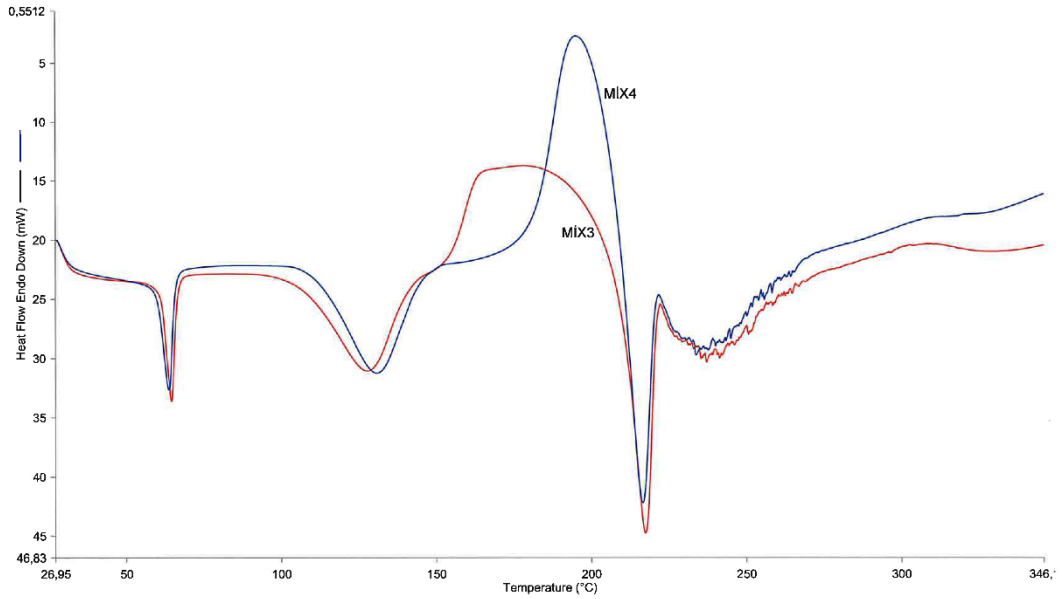

Figure 4.18. Thermogram of HPMC 15K formulations; mix 3 drug-free tablet, mix 4 drug-loaded tablet

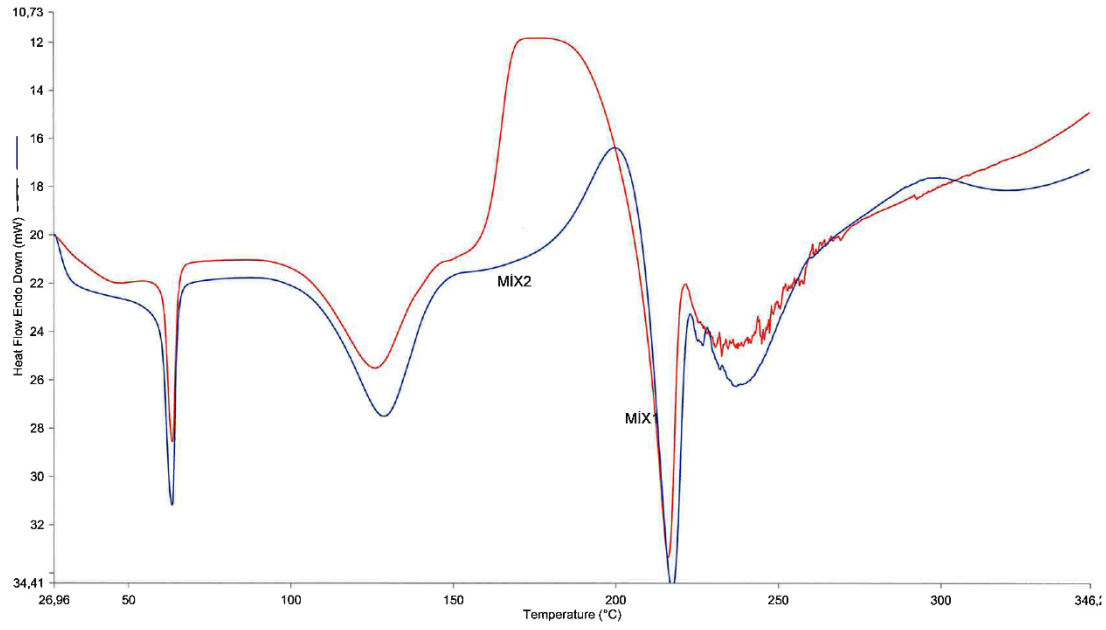

Figure 4.19. Thermograms of HPMC 100K formulations; mix 1 drug-free tablet, mix 2 drug-loaded tablet

5. DISCUSSION AND CONCLUSION

5.1. Identification of Repaglinide using ATR-FTIR/ DSC

Comparison of the IR spectrum obtained through our experiment and the one obtained from literature (Olteanu et al., 2014) shows near identical symmetry of peaks and valley ensuring the authenticity of our API. DSC thermograph showed sharp valley of melting point range (130-138°C) which is in line with the reported repaglinide melting point by PubChem.

5.2. Optimizing of Printing Ink/ Paste:

One of the first and major challenges of Semi-Solid Extrusion printing SSE is forming a paste that is printable, i.e., the paste should possess the viscosity, continuity and elasticity to be extruded from the nozzle as a continuous thin filament. The filament/paste should also have the appropriate moisture content to be extrudable and be firm enough to maintain its structural integrity and not crumble down under its own weight during and after printing. Finally, the prints should be able to harden after printing.

Published literature discussed assessment and ways to predict paste extrudability and printability (60-61). However, when it comes to pharmaceutical preparation, challenges arise due to the numerous component that is usually present in a formulation (Binder, Filler, Plasticizer, release modifier, etc.). Each is having different rheological properties and is needed to be present in a specific concentration to perform their desired function, hence the challenges lie in finely adjusting the ink to arrive at the perfect blend that harness the physical properties needed for perfect extrusion, printability and later hardening. For our experiments, we optimized the ink by adjusting the constituents' percentages, liquid binder quantity and the printing settings.

Excipients

HPMC percentage in the two formulations were kept fixed. Amount of Lactose and PEG were adjusted to reach the perfect extrudable paste. Increasing PEG percentage results in waxy and soft paste. Tablets that were printed using high percentage of PEG had deformed design, where the bottom layers spread in diameter

due to the soft, waxy texture. Tablets with higher PEG content would normally crumble in hand while handling.

Liquid Binder Quantity

Quantity of binder has a major effect on paste qualities, which in turn determine the final quality of tablet. We experienced with different quantities of binder for the same amount of dry mix.

As amount of the binder increased, the paste soften and become more adhesive. A soft paste tends to ooze out of the needle uncontrollably during the printing process; this causes deposition of extra material resulting in a defective and unpleasant structure. Additionally, an extremely soft paste does not have enough mechanical strength to support the top layers and will collapse into a cone like shape such as in Figure 5.1.

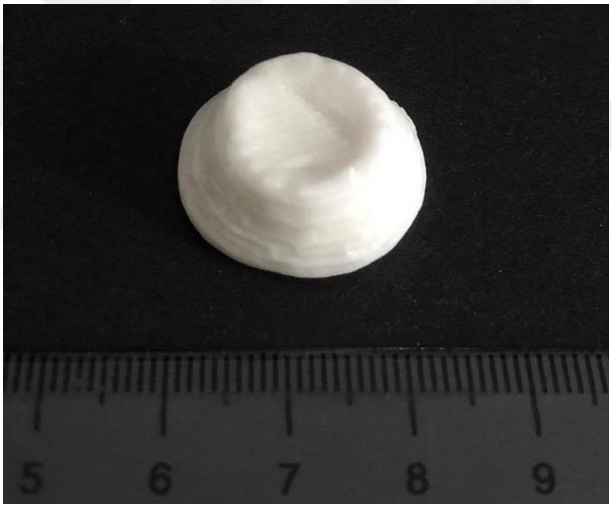

Figure 5.1. 3D printed tablet of crumbling cone-like shape due to the softness of paste/ink

On the other hand, a dry paste will encounter a different set of issues, namely, a dry paste is harder to be filled into the printer cartridge causing air to be entrapped within. During printing, this results in missing strands due to air entrapment and bursting of chunks of paste at one time. Furthermore, using less liquid results in strands that vary in diameter (Figure 5.2). This may be attributed to insufficient hydration leaving some parts of the paste wetter than others, which may also cause high variation

in tablets weight within the same batch. Poor hydration may also be the result of insufficient mixing of paste.

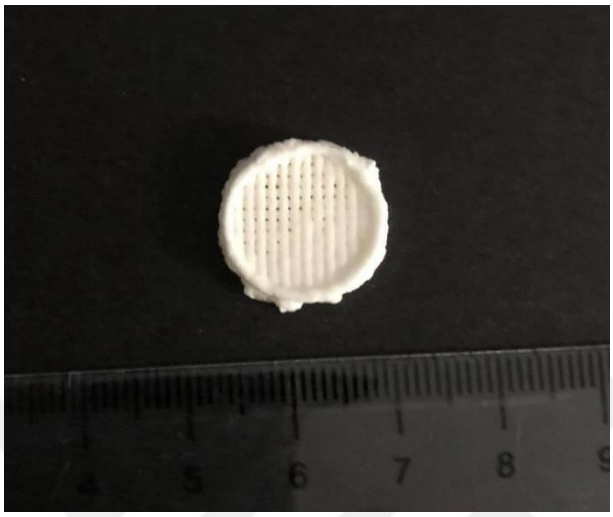

Figure 5.2. Inconsistent strand diameter attributed to poor hydration of paste

Filling

The aim of a good filling is to have the paste loaded perfectly into the cartridge with no air entrapped. The blunger should be in contact with the paste so the pressure could be distributed equally on the surface. Filling is closely affected and controlled by paste properties, a dry paste will spread less when loaded causing air to be trapped inside, while an extremely adhesive paste may stick to the surfaces or the blunger during printing and may be lifted with it when the pressure halt during printing. Ultimately, a bad filling may lead to two major issues when printing; air printing, is what we call air passing through the needle causing the loss of strands in the print, and sudden bursting of chunks of paste. Good filling should lead to continuous extruded strands throughout the whole printing process.

Pressure and Speed of printing

Pressure and speed are the two most important parameters for printing settings. Together pressure and speed control how much paste is deposited at one space at an instance. Naturally, dryer paste requires higher pressure and lower speed and vice versa. In this sense, liquid quantity adjustment requires adjustment of settings, for example, in our study 100K formulation required more liquid binder than 15K formulation which required us to increase speed from 2 to 4 mm/s. Additionally, since both pressure and speed control how much material is deposited, arriving at perfect value is essential to have perfect shape of the design. Excess or insufficient material deposition produces an unpleasant or deformed structure. Figure 5.3-5.4 illustrate our gradual experimental approach to optimization of ink/paste and printing settings to arrive at the final design.

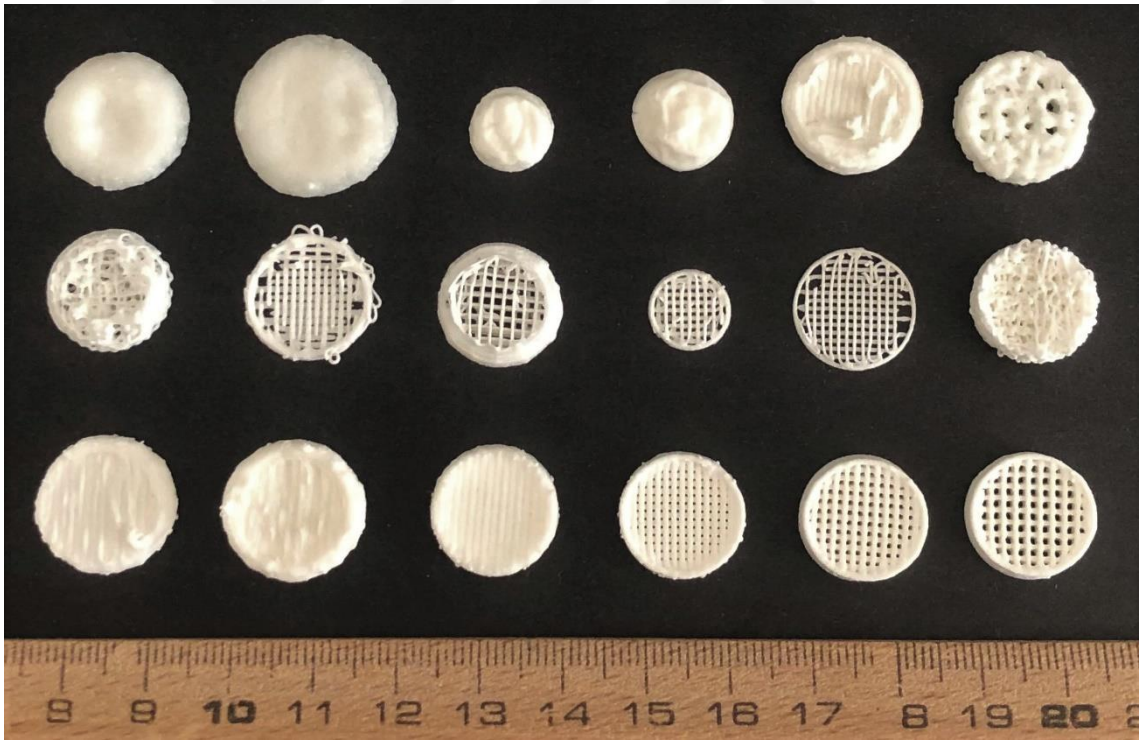

Figure 5.3. Image of the tablets resulting from the gradual experimental optimization of paste/ink and printing settings (top view)

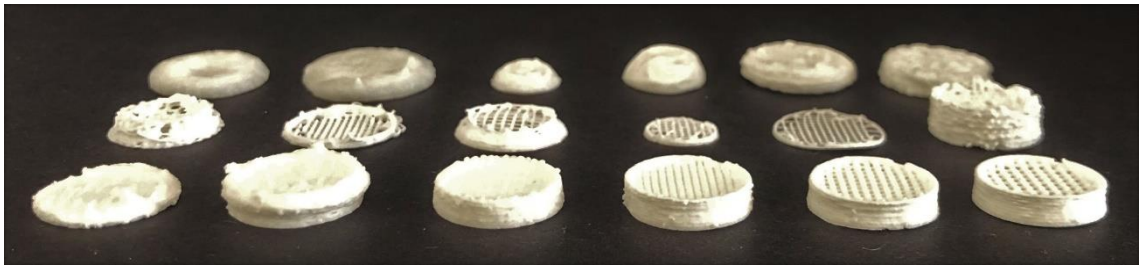

Figure 5.4. Image of the tablets resulting from the gradual experimental optimization of paste/ink and printing settings (side view)

5.3. Evaluative Studies on Tablets

5.3.1. Hardness

All tablets were evaluated for their mechanical properties. Hardness test results revealed values range between 0.6 and 5.2 Kilopose (Kp). As expected, more compact designs exhibited higher hardness value and vice versa. 15K formulation (1.0 and 1.3SD) returned slightly higher average hardness when compared to100K formulation (Figure 4.11). This could be attributed to using less amount of liquid binder in 15K formulation than 100K (1.6 mL and 1.8 mL respectively). Hardness is an un-official test that is largely employed by drug manufacturers to provide an indication on the tablets' resistance to breakage during manufacturing, packaging and shipping as well as proper disintegration after swallowing (62). Harder tablets could show slower disintegration and release when compared to softer tablets. During our experiment of semi-solid extrusion printing, control of tablet hardness could be achieved through compactness of design as well as liquid binder content, our control over the latter is extremely limited, as to arrive at an optimized printable paste, an exact amount of liquid must be used. Generally, we believe that 3DP tablets exhibit lower hardness values when compared to conventional tablets due to lack of compression force used in tablet punches. This has led to the employment of 3DP in rapidly dispersed tablets (63,6).

5.3.2. Weight Variation

Weight of the tablets alongside hardness are the two most deviated values. When hardness is plotted against weight, we can observe increase in hardness as weight increases as shown in Figure 5.5. Naturally, more compact designs exhibit higher weight since more material is deposited in one place, which may be an additional reason for their slower rupture time.

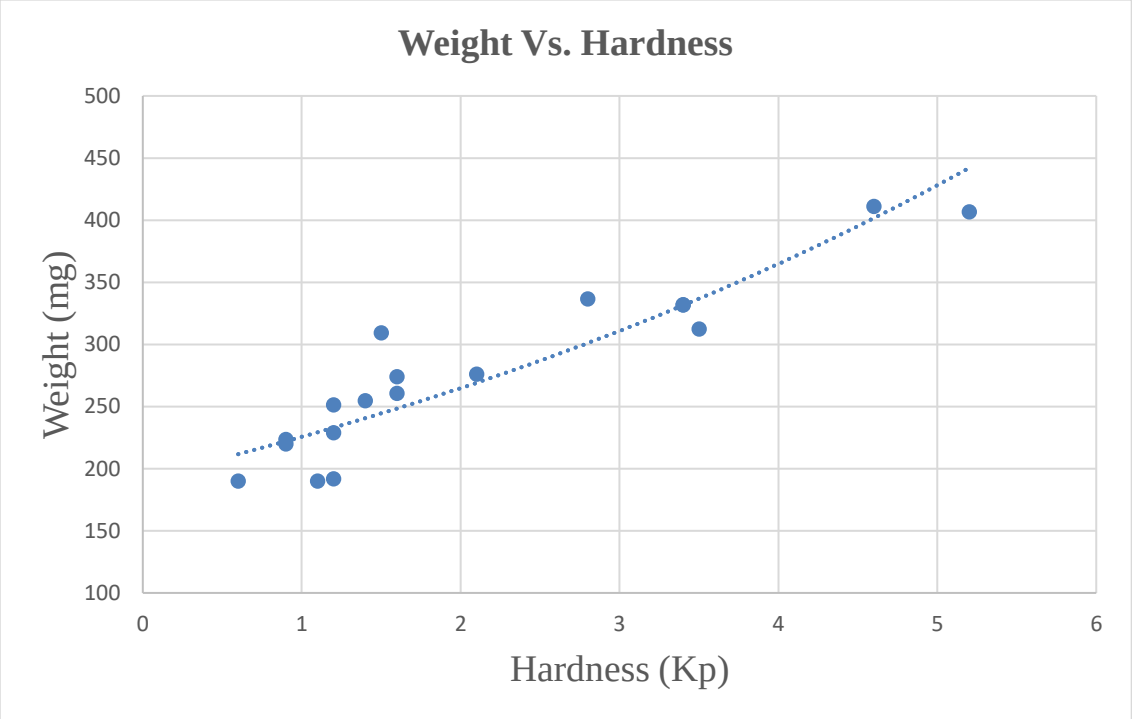

Figure 5.5. Weight of tablets plotted against hardness values.

Undesirable weight variation is observed for the same tablet. Tablets produced of same batch exhibit very small or negligible weight variation. However, tablets produced of different batches may show larger variation in weight. This could be due to variation in environmental factors surrounding the making of the batch such as; slight difference in amount of liquid binder, more or less exposure to air and humidity leading to dryer or wetter paste which in turn results in filament containing less or more of the excipients. Other factors could be related to the printer itself, Khaled et. al. (54)

reported such issue while using smaller scale bioprinter and attributed the variation to lack of specialized software for deposition control.

5.3.3. Friability

Test of the 18 tablets has returned an average loss in mass of 0.8%. Only 3 tablets exhibited loss of more than 1% which is the pharmacopeial limit (1.09, 1.27, and 1.11%) for 100K1.3SD, 1.6SD and 15K1.0SD respectively. Friability is intended to demonstrate tablet tendency for chipping or breakage during handling and manufacturing. Since our tablets is mostly intended for personalized therapy at clinical settings, rough handling is unlikely. Nevertheless, only 3 out of the 18 tablets were slightly over the pharmacopeial friability standards of 1% weight loss. The random distribution of values across the graph in Figure 4.13, indicates that differences in pore size did not impact friability. It is important to note that none of the tablets which underwent friability testing exhibited chipping, crumbling or breakage, and all tablets exhibited structural integrity during handling and testing.

5.3.4. Thickness and Diameter

The average thickness and diameter of all the tablets were 3.24, and 15.13 mm, respectively, with negligible variation proving that our process can repeatably produce tablets of structural integrity and fixed dimensions.

All the mechanical attributes of the 3D printed tablets are plotted in relation to each other in Figure 5.6. 15K tablets exhibit higher weight and thickness where both 1.0SD and 1.3SD came first, this is the results of using less amount of liquid binder which generates dryer strands. Having less water in the formulation causes the strands to be harder and the tablets to be heavier. In addition, harder strands with less liquid content could dry faster during the printing process causing the following layer to stack higher. Nevertheless, the deviation in tablet thickness is negligible.

Hardness varied largely among the different tablets, and appears to be majorly governed by weight and tablet design. Although 15K1.0SD tablets exhibited on average higher weight, they showed less hardness value when compared to 100K1.0SD tablets, indicating that compactness of the design has resulted in harder tablets even when compared to heavier more porous ones. It is worth noting that for the dissolution test,

tablets were taken from more than one batch and of near similar weight in order to isolate the effect of design on drug release.

The occasional variation in tablets hardness and weight is often resulted from batch-to-batch difference. This problem is previously stated by Khalid et al. (54), the batch-to-batch difference could be the result of environmental factors such as humidity and laboratory temperature which can cause one paste to be dryer or wetter than the next one. These differences may be minimized by more strict control over paste formulation techniques and loading. Khalid et al, stated the need for a more controlled extrusion through a specialized software as a solution for batch-to-batch variation.

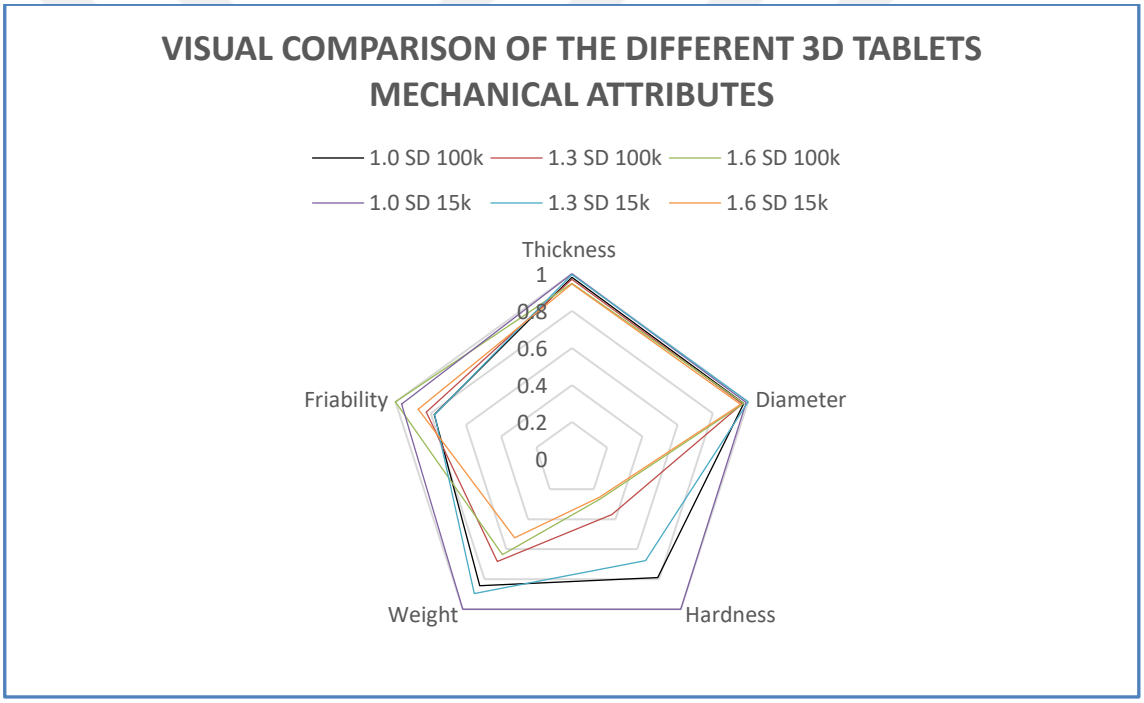

Figure 5.6. Visual comparison of the different mechanical attributes of the 3D printed tablets

5.3.5. Dissolution and Release

All tablets exhibited sustained release behavior over 12-hour period. The graph (Figure 4.17) indicates that the release behavior and maximum amount of drug released is governed by two factors; the design of the tablets, i.e., pore size, and grade of HPMC

within the formulation. Tablets of smaller pore size is found to have lower rate of release, and less total amount released when compared to tablets of same formulation with larger pores. Formulation wise, HPMC 100K formulation tablets showed slower and more limited release when compared to HPMC 15K tablet of same porosity. Given these results, Porosity through design fabrication and formulation choices can tune a designed release behavior most suitable to present need.

In addition to the rate and overall extent of release, porosity and grade of polymer controlled how long a tablet remained intact. Upon contact with dissolution medium, tablets formed gel-like mass which could be attributed to the gel forming propriety of HPMC, it is worth noting that none of the tablets disintegrated upon insertion in medium nor experienced burst release (Figure 4.17).

Unsurprisingly, tablets with the most compact design and higher polymer grade remained intact for longer period and vice versa. Upon observation of tablets during dissolution, HPMC 100K1.0SD remained unbroken for the entirety of the test while the rest of the tablets experienced breakage in the gel structure around the following times; HPMC100K1.3SD ≈ 5 hr., 1.6SD ≈ 4 hr., HPMC15K1.0SD ≈ 8 hr., 1.3SD ≈ 4 hr., 1.6SD ≈ 1 hr. The breakage time effect can be seen reflected on the dissolution profile Figure 4.17, where slight upward shift in the release plot can be seen around these times. This could open up the possibility to design a timed pulsatile release tablets form through the control of the tablets filling design.

According to these findings and observation of tablets during dissolution, we theorize that dissolution was controlled by design and polymer viscosity grade, upon introducing the tablet into the medium, they immediately form a gel mass that is similar in all tablets. However, inter-structural grooves within the gel formed because of the perforated design remained and has facilitated breakage and dissolution by introducing week points within the gel structure as well as offering thin areas of gel for the medium to penetrate more easily and the drug to be released.

The clear release behavior adjustability that was achieved through design fabrication as well as polymer choice provides personalization opportunities of medication, a more compact design with slower release may be offered as a single daily dose medication, while lesser compacted tablets may be offered as two and three-times daily dose. The enhanced release profile (increased rate and quantity) attained by

increasing tablet porosity clearly indicates that the dissolution of highly water-insoluble drugs such as repaglinide can be enhanced through tablet design fabrication.

5.3.6. Comparison of Dissolution Profiles

Similarity and Difference Factors

As seen from Table 4.8 showing the f_2 values, within the 15K and 100K formulations all the pairs are different. These tablets are different in their pore size made possible through strand distance (SD) control of tablet filling. When we compared tablets with different formulations but same SD, 15K1.6 vs 100K1.6 and 15K1.3 vs 100K 1.3SD, results showed that these tablets are different. Nevertheless, 15K1.0 vs 100K1.0 showed similarity with an f_2 value of 52.74. This led us to believe that fabrication of tablet design perforation had far higher effect on release behavior than polymer grade. Also, these results demonstrate that a perforated tablet could enhance the dissimilarity generated by different polymers, this can be observed when comparing the f_2 values of perforated tablet of same SD and different polymers to their corresponding more compact tablets as reported in section (3) of Table 4.8. This may be the results of the enhanced swelling of polymer made possible through surface area enhancement and inner pathways for solvent diffusion. Finally, from visual observations of graphs, 15K1.3 & 100K1.6 and 15K1.0 & 100K1.3 were suspected to be similar which was actually the case as shown by their f_2 values of 75.10 and 60.81, respectively. These tablets with different formulation and different porosity exhibiting similarity of dissolution profile shows interacting multiple factors playing their roles.

When evaluated by the f_1 values, only 15K1.3 & 100K1.6 pair showed similarity with 6.74, in conformity with f_2 value of 75.1. The pairs 15K1.0 & 100K1.0 (52.74) and 15K1.0 & 100K1.3 (60.81) were shown similar by their f_2 values but their f_1 values were 28.93 and 19.89, respectively. When judged on the f_1 scale of 0-15 for similarity, these two pairs are different, one being just outside the upper limit of 15. However, the equation for f_1 (section 3.3.8) is a directly proportional type whereas that for f2 is a logarithmic function and this is considered more sensitive to differentiate one profile from another. From this point of view, 19.89 and 28.93, being very close to 15, do not signify gross dissimilarity and therefore do not completely oppose the outcome of f_2 similarity. On the other hand, accepting the f_1 outcome, that is, the 15K1.0 & 100K1.0

and 15K1.0 & 100K1.3 pairs are different, makes practical sense as the 15K1.0 & 100K1.0 pair contained different polymers and 15K1.0 & 100K1.3 pair differs both in polymer and SD parameters.

Dissolution Efficiency

Dissolution efficiency is defined as the area under the dissolution curve up to a certain time, t, expressed as a percentage of the area of the rectangle described by 100% dissolution in the same time (58). Area under a specific dissolution profile in 12 h actually compares to a fixed value of 1200. We can rank order these six formulations by the DE values (2nd column in Table 4.9), from highest to lowest efficiency, as: 15K1.6 >100K1.6 > 15K1.3 >100K1.3 > 15K1.0 >100K1.0. Clearly higher empty space in the tablets (SD values 1.6) showed higher efficiency, lower space (1.0SD) lower efficiency and medium space (1.3SD) in the middle. Highly porous structure in the tablets negates the effect of high viscosity polymer 100K, as 100K1.6 showed higher dissolution efficiency than 15K1.3 and 15K1.0 which contain low viscosity polymer but low level of porosity as well. As such, poorly soluble drug can be dissolved faster by increasing perforation in the system; and formulation and printing parameter can be considered in combination to achieve a desired dissolution rate.

It is also interesting to compare AUCs of individual formulation to the AUC of another formulation (normally a formulation showing higher dissolution rate). Within 15K formulations, 15K1.6 showed the highest AUC; in comparison to this, 15K1.3 and 15K1.0 returned (62.72, and 36.48%, respectively). Similar results were seen within 100K formulations. When comparison was performed among all the six tablets, 15K1.6 had the highest AUC of 733.42. Other AUCs are presented on the last column of Table 4.9 as its percentage. As was expected, we see the same rank order of 15K1.6 >100K1.6 > 15K1.3 >100K1.3 > 15K1.0 >100K1.0.

Two-Way Analysis of Variance ANOVA

As is clear from the Table 4.11, the dissolution values are significantly different right from the 1h point. Two hour and 4h values are significantly different as well implying that later data points are not required to be analyzed. The difference among 1.0, 1.3, 1.6 SD (among SD) were significant as well as the difference between 100K and 15K (formulations). There is clearly significant interaction between

formulations and SD (interaction). The data also indicates that perforation design difference had more significant impact on release than formulation difference.

5.3.7. Modelling of Drug Release Kinetics

Interpretation of n-values depend on the type of dosage form like thin film, sphere and cylindrical tablets. The shapes of our 3D printed tablets were close to cylindrical tablets, though in fact they were cylindrical with different degree of perforations. Therefore, n-values reported for cylindrical tablets were taken into consideration to evaluate the release mechanisms. For cylindrical tablets, $n = 0.45$ corresponds to a Fickian diffusion mechanism, other mechanisms are classified as non-Fickian which are; $0.45 < n < 0.89$ to Anomalous transport, $n = 0.89$ to Case II transport, and $n > 0.89$ to super case II transport (59, 64).

In light of the release exponent (n) results calculated by Korsmeyer-Peppas model fitting and our understanding of tablet design we may predict the mechanism that governed drug release from tablets matrix.

According to the Korsmeyer-Peppas model, drug release can be classified into Fickian and non-Fickian release which indicates two major mechanism of drug release from polymeric dosage forms; relaxation of polymer chain (swelling) and solvent diffusion. Fickian release is governed by diffusion of solvent as it is far higher than polymer chain relaxation, whereas non-Fickian can be further classified into (Class II, Anomalous, and Super Class II). In Class II release, the solvent diffusion through the jellified layer is higher than polymer relaxation of the gel-vitreous interface, this makes swelling and relaxation of polymer the rate limiting step of this kind of system. Anomalous release is when diffusion and polymer relaxation have similar magnitude (the polymer swells gradually as the solvent penetrate the system). Super Case II is an extreme case where the velocity of solvent diffusion is way higher than polymer relaxation causing tension and breakage in polymer system. the matrix experience accelerated swelling due to rapid penetration of solvent; this causes the inner gel-vitreous interface to move inward rapidly. This rapid penetration combined with increasing pressure by the expanding outer gel layer of the matrix results in breakage of the inner nucleus. (65).

In exemption of 100K1.0SD, all our tablets exhibited super class II release (Table 4.10). This is due to the perforated design of our tablets. The pores, upon insertion in medium, provided additional pathways for solvent penetration, making new surfaces for jelling and drug diffusion. This causes rapid relaxation of polymer chains and jelling on the outer and inner surfaces of the tablet. This in turn causes the release of drug to be predominately controlled by solvent diffusion rather than polymer swelling, as vitreous-gel layer was lost, most polymer has swelled and the tablets had experienced rupture due to buildup of inner pressure facilitated by the perforation. On the other hand, 100K1.0SD tablet had exhibited Anomalous release where polymer swelling and solvent diffusion have similar magnitudes. This behavior can be explained by the same concept where the smaller pore size and high polymer viscosity grade had limited solvent diffusion into the core of the tablet, sustaining the vitreous-gel interface and shifting the release mechanism into Anomalous behavior.

As perforation size increases and polymer grade decreases, a pattern of increased release exponent value (n) can be detected (Table 4.10). This may be an indication of the role of pore size enlargement in shifting the release mechanism towards solvent diffusion. However, 15K1.6SD appear to not follow this rule. We could theorize that the rapid breakage of gel structure of this tablet (≈ 1hr., see section 5.3.5) as observed during the dissolution test, had resulted in the quick transformation to expanded thin, homogenous and continuous gel body. The rapid loss of the geometrical cylindrical shape may have caused the (n) value of this tablet to drop below the predicted pattern observed by the other tablets.

5.3.8. Assessment of Drug-Excipient Interaction

The thermograms for the formulation with and without drug are practically the same with very slight variation in the peaks position as shown in Figure 4.18 and 4.19. Such minor variations are often seen with the repetition of measurements of the same samples. Therefore, the possibility of any interaction of drug with excipient were excluded.

5.4. Conclusion

In conclusion, this study had successfully demonstrated production of printing paste using traditional pharmaceutical excipients including two different polymers, printing of complex design tablets that is otherwise not possible using traditional manufacturing methods. Evaluation of these tablets has shown satisfactory mechanical integrity even though they had visibly different degree of perforations. Evaluation of tablets performance revealed that dissolution rates of the drug was tunable mainly by the levels of perforation within the tablet structure making this process a viable option for personalized medication. Furthermore, tablet perforation and polymer control has shown enhanced dissolution of a poorly water-soluble drug, repaglinide.

6. REFERENCES

1. Matijašić G, Gretić M, Vinčić J, Poropat A, Cuculić L, Rahelić T. Design and 3D printing of multi-compartmental PVA capsules for drug delivery. *Journal of Drug Delivery Science and Technology*. 2019;52:677-686. doi:10.1016/j.jddst.2019.05.037
2. Jamróz, W., Kurek, M., Łyszczarz, E., Szafraniec, J., Knapik-Kowalczuk, J., Syrek, K., Paluch, M. and Jachowicz, R., 2021. 3D printed orodispersible films with Aripiprazole.
3. Genina N, Holländer J, Jukarainen H, Mäkilä E, Salonen J, Sandler N. Ethylene vinyl acetate (EVA) as a new drug carrier for 3D printed medical drug delivery devices. *European Journal of Pharmaceutical Sciences*. 2016;90:53-63. doi:10.1016/j.ejps.2015.11.005
4. Holländer J, Genina N, Jukarainen H, et al. Three-Dimensional Printed PCL-Based Implantable Prototypes of Medical Devices for Controlled Drug Delivery. *Journal of Pharmaceutical Sciences*. 2016;105(9):2665-2676. doi:10.1016/j.xphs.2015.12.012
5. Fu J, Yu X, Jin Y. 3D printing of vaginal rings with personalized shapes for controlled release of progesterone. *International Journal of Pharmaceutics*. 2018;539(1-2):75-82. doi:10.1016/j.ijpharm.2018.01.036
6. Fina F, Madla CM, Goyanes A, Zhang J, Gaisford S, Basit AW. Fabricating 3D printed orally disintegrating printlets using selective laser sintering. *International Journal of Pharmaceutics*. 2018;541(1-2):101-107. doi:10.1016/j.ijpharm.2018.02.015
7. Clark EA, Alexander MR, Irvine DJ, et al. 3D printing of tablets using inkjet with UV photoinitiation. *International Journal of Pharmaceutics*. 2017;529(1-2):523-530. doi:10.1016/j.ijpharm.2017.06.085
8. Ghanizadeh Tabriz A, Nandi U, Hurt AP, et al. 3D printed bilayer tablet with dual controlled drug release for tuberculosis treatment. *International Journal of Pharmaceutics*. 2021;593:120147. doi:10.1016/j.ijpharm.2020.120147
9. Vaz VM, Kumar L. 3D Printing as a Promising Tool in Personalized Medicine. *AAPS PharmSciTech*. 2021;22(1). doi:10.1208/s12249-020-01905-8

10. Mandić Z, Gabelica V. Ionization, lipophilicity and solubility properties of repaglinide. *Journal of Pharmaceutical and Biomedical Analysis*. 2006;41(3):866-871. doi:10.1016/j.jpba.2006.01.056
11. Pandey SS, Patel MA, Desai DT, et al. Bioavailability enhancement of repaglinide from transdermally applied nanostructured lipid carrier gel: Optimization, in vitro and in vivo studies. *Journal of Drug Delivery Science and Technology*. 2020;57:101731. doi:10.1016/j.jddst.2020.101731
12. Foster SL, Petrie SR, Mischoulon D, Fava M. Personalized Medicine. *The Massachusetts General Hospital Guide to Depression*. 2018:109-121. doi:10.1007/978-3-319-97241-1_8
13. DeFronzo RA, Ferrannini E, Groop L, et al. Type 2 diabetes mellitus. *Nature Reviews Disease Primers*. 2015;1(1). doi:10.1038/nrdp.2015.19
14. Collins FS, Varmus H. A New Initiative on Precision Medicine. *New England Journal of Medicine*. 2015;372(9):793-795. doi:10.1056/nejmp1500523
15. Horwitz RI, Cullen MR, Abell J, Christian JB. (De)Personalized Medicine. *Science*. 2013;339(6124):1155-1156. doi:10.1126/science.1234106
16. Meyer JM, Ginsburg GS. The path to personalized medicine. *Current Opinion in Chemical Biology*. 2002;6(4):434-438. doi:10.1016/s1367-5931(02)00340-x
17. Kautzky-Willer A, Harreiter J, Pacini G. Sex and Gender Differences in Risk, Pathophysiology and Complications of Type 2 Diabetes Mellitus. *Endocrine Reviews*. 2016;37(3):278-316. doi:10.1210/er.2015-1137
18. Zhu X, Li H, Huang L, Zhang M, Fan W, Cui L. 3D printing promotes the development of drugs. *Biomedicine & Pharmacotherapy*. 2020;131:110644. doi:10.1016/j.biopha.2020.110644
19. Martinez PR, Goyanes A, Basit AW, Gaisford S. Influence of Geometry on the Drug Release Profiles of Stereolithographic (SLA) 3D-Printed Tablets. *AAPS PharmSciTech*. 2018;19(8):3355-3361. doi:10.1208/s12249-018-1075-3
20. Scoutaris N, Ross SA, Douroumis D. 3D Printed "Starmix" Drug Loaded Dosage Forms for Paediatric Applications. *Pharmaceutical Research*. 2018;35(2). doi:10.1007/s11095-017-2284-2

21. Goyanes A, Buanz ABM, Basit AW, Gaisford S. Fused-filament 3D printing (3DP) for fabrication of tablets. *International Journal of Pharmaceutics*. 2014;476(1-2):88-92. doi:10.1016/j.ijpharm.2014.09.044
22. Culy CR, Jarvis B. Repaglinide. *Drugs*. 2001;61(11):1625-1660. doi:10.2165/00003495-200161110-00008
23. Milner Z, Akhondi H. Repaglinide. Treasure Island, FL: StatPearls Publishing; 2021. https://www.ncbi.nlm.nih.gov/books/NBK559305/. Accessed June 02, 2021.
24. Yin L-F, Huang S-J, Zhu C-L, et al. In vitro and in vivo studies on a novel solid dispersion of repaglinide using polyvinylpyrrolidone as the carrier. *Drug Development and Industrial Pharmacy*. 2012;38(11):1371-1380. doi:10.3109/03639045.2011.652635
25. Nanjwade BK, Varia PJ, Kadam VT, Srichana T, Kamble MS. Development and evaluation of nanoemulsion of repaglinide. *Nanotechnol. Nanomed.* 2013;1(2):1-8.
26. Karami Z, Saghatchi Zanjani MR, Nasihatsheno N, Hamidi M. Improved oral bioavailability of repaglinide, a typical BCS Class II drug, with a chitosan-coated nanoemulsion. *Journal of Biomedical Materials Research Part B: Applied Biomaterials*. 2019;108(3):717-728. doi:10.1002/jbm.b.34426
27. Zhu Z, Yang T, Zhao Y, Gao N, Leng D, Ding P. A simple method to improve the dissolution of repaglinide and exploration of its mechanism. *Asian Journal of Pharmaceutical Sciences*. 2014;9(4):218-225. doi:10.1016/j.ajps.2014.06.004
28. Ngo TD, Kashani A, Imbalzano G, Nguyen KTQ, Hui D. Additive manufacturing (3D printing): A review of materials, methods, applications and challenges. *Composites Part B: Engineering*. 2018;143:172-196. doi:10.1016/j.compositesb.2018.02.012
29. Su A, Al'Aref SJ, Mosadegh B, Dunham S, Al'Aref SJ. History of 3D Printing. In: Min J, ed. *3D Printing Applications in Cardiovascular Medicine*. New York, NY: Academic Press; 2018:1-10.

30. Savini A, Savini GG. A short history of 3D printing, a technological revolution just started. *2015 ICOHTEC/IEEE International History of High-Technologies and their Socio-Cultural Contexts Conference (HISTELCON)*. 2015. doi:10.1109/histelcon.2015.7307314
31. Sachs EM, Haggerty JS, Cima MJ, Williams PA. Three-dimensional printing techniques. April 1993.
32. Horvath J. (2014) A Brief History of 3D Printing. In: Mastering 3D Printing. Apress, Berkeley, CA. https://doi.org/10.1007/978-1-4842-0025-4_1
33. Zhang B, Luo Y, Ma L, et al. 3D bioprinting: an emerging technology full of opportunities and challenges. *Bio-Design and Manufacturing*. 2018;1(1):2-13. doi:10.1007/s42242-018-0004-3
34. Mironov V, Boland T, Trusk T, Forgacs G, Markwald RR. Organ printing: computer-aided jet-based 3D tissue engineering. *Trends in Biotechnology*. 2003;21(4):157-161. doi:10.1016/s0167-7799(03)00033-7
35. Ouyang L. 3D Bioprinting and Bioink: Background. *Study on Microextrusion-based 3D Bioprinting and Bioink Crosslinking Mechanisms*. 2019:7-23. doi:10.1007/978-981-13-9455-3_2
36. Jamróz W, Szafraniec J, Kurek M, Jachowicz R. 3D Printing in Pharmaceutical and Medical Applications – Recent Achievements and Challenges. *Pharmaceutical Research*. 2018;35(9). doi:10.1007/s11095-018-2454-x
37. FDA. Application number: 207958Orig1s000 approval letter.; 2018 March 26. https://www.accessdata.fda.gov/drugsatfda_docs/nda/2015/207958Orig1s000Approv.pdf
38. Kadry H, Al-Hilal TA, Keshavarz A, et al. Multi-purposable filaments of HPMC for 3D printing of medications with tailored drug release and timed-absorption. *International Journal of Pharmaceutics*. 2018;544(1):285-296. doi:10.1016/j.ijpharm.2018.04.010
39. Melocchi A, Parietti F, Maroni A, Foppoli A, Gazzaniga A, Zema L. Hot-melt extruded filaments based on pharmaceutical grade polymers for 3D printing by fused deposition modeling. *International Journal of Pharmaceutics*. 2016;509(1-2):255-263. doi:10.1016/j.ijpharm.2016.05.036

40. Sadia M, Arafat B, Ahmed W, Forbes RT, Alhnan MA. Channelled tablets: An innovative approach to accelerating drug release from 3D printed tablets. *Journal of Controlled Release*. 2018;269:355-363. doi:10.1016/j.jconrel.2017.11.022
41. Khaled SA, Alexander MR, Irvine DJ, et al. Extrusion 3D Printing of Paracetamol Tablets from a Single Formulation with Tunable Release Profiles Through Control of Tablet Geometry. *AAPS PharmSciTech*. 2018;19(8):3403-3413. doi:10.1208/s12249-018-1107-z
42. Stanojević G, Medarević D, Adamov I, Pešić N, Kovačević J, Ibrić S. Tailoring Atomoxetine Release Rate from DLP 3D-Printed Tablets Using Artificial Neural Networks: Influence of Tablet Thickness and Drug Loading. *Molecules*. 2020;26(1):111. doi:10.3390/molecules26010111
43. Martinez PR, Goyanes A, Basit AW, Gaisford S. Influence of Geometry on the Drug Release Profiles of Stereolithographic (SLA) 3D-Printed Tablets. *AAPS PharmSciTech*. 2018;19(8):3355-3361. doi:10.1208/s12249-018-1075-3
44. Öblom H, Zhang J, Pimparade M, et al. 3D-Printed Isoniazid Tablets for the Treatment and Prevention of Tuberculosis—Personalized Dosing and Drug Release. *AAPS PharmSciTech*. 2019;20(2). doi:10.1208/s12249-018-1233-7
45. Khaled SA, Burley JC, Alexander MR, Yang J, Roberts CJ. 3D printing of five-in-one dose combination polypill with defined immediate and sustained release profiles. *Journal of Controlled Release*. 2015;217:308-314. doi:10.1016/j.jconrel.2015.09.028
46. Khaled SA, Burley JC, Alexander MR, Yang J, Roberts CJ. 3D printing of tablets containing multiple drugs with defined release profiles. *International Journal of Pharmaceutics*. 2015;494(2):643-650. doi:10.1016/j.ijpharm.2015.07.067
47. Pereira BC, Isreb A, Isreb M, Forbes RT, Oga EF, Alhnan MA. Computer-aided Drug Design: Additive Manufacturing of a Point-of-Care "Polypill:" Fabrication of Concept Capsules of Complex Geometry with Bespoke Release against Cardiovascular Disease (Adv. Healthcare Mater. 13/2020). *Advanced Healthcare Materials*. 2020;9(13):2070042. doi:10.1002/adhm.202070042

48. Maroni A, Melocchi A, Parietti F, Foppoli A, Zema L, Gazzaniga A. 3D printed multi-compartment capsular devices for two-pulse oral drug delivery. *Journal of Controlled Release*. 2017;268:10-18. doi:10.1016/j.jconrel.2017.10.008
49. El Aita I, Breitkreutz J, Quodbach J. On-demand manufacturing of immediate release levetiracetam tablets using pressure-assisted microsyringe printing. *European Journal of Pharmaceutics and Biopharmaceutics*. 2019;134:29-36. doi:10.1016/j.ejpb.2018.11.008
50. Siyawamwaya M, du Toit LC, Kumar P, Choonara YE, Kondiah PPPD, Pillay V. 3D printed, controlled release, tritherapeutic tablet matrix for advanced anti-HIV-1 drug delivery. *European Journal of Pharmaceutics and Biopharmaceutics*. 2019;138:99-110. doi:10.1016/j.ejpb.2018.04.007
51. Olteanu AA, Aramă C-C, Radu C, Mihăescu C, Monciu C-M. Effect of β-cyclodextrins based nanosponges on the solubility of lipophilic pharmacological active substances (repaglinide). *Journal of Inclusion Phenomena and Macrocyclic Chemistry*. 2014;80(1-2):17-24. doi:10.1007/s10847-014-0406-6
52. He W, Wu M, Huang S, Yin L. Matrix tablets for sustained release of repaglinide: Preparation, pharmacokinetics and hypoglycemic activity in beagle dogs. *International Journal of Pharmaceutics*. 2015;478(1):297-307. doi:10.1016/j.ijpharm.2014.11.059
53. VALIDATION OF ANALYTICAL PROCEDURES: TEXT AND METHODOLOGY, ICH Harmonised Tripartite Guideline, November 2005.
54. Khaled SA, Burley JC, Alexander MR, Roberts CJ. Desktop 3D printing of controlled release pharmaceutical bilayer tablets. *International Journal of Pharmaceutics*. 2014;461(1-2):105-111. doi:10.1016/j.ijpharm.2013.11.021
55. Abd-Allah FI, Dawaba HM, Ahmed AM. Preparation, characterization, and stability studies of piroxicam-loaded microemulsions in topical formulations. *Drug Discov Ther*. 2010 Aug 1;4(4):267-75.
56. Moore JW, Flanner HH. Mathematical comparison of dissolution profiles. *Pharmaceutical technology*. 1996;20(6):64-74

57. Xie F, Ji S, Cheng Z. In vitro dissolution similarity factor (f2) and in vivo bioequivalence criteria, how and when do they match? Using a BCS class II drug as a simulation example. *European Journal of Pharmaceutical Sciences*. 2015;66:163-172. doi:10.1016/j.ejps.2014.10.002
58. Khan KA. The concept of dissolution efficiency. *Journal of Pharmacy and Pharmacology*. 1975;27(1):48-49. doi:10.1111/j.2042-7158.1975.tb09378.x
59. Siepmann J. Modeling of drug release from delivery systems based on hydroxypropyl methylcellulose (HPMC). *Advanced Drug Delivery Reviews*. 2001;48(2-3):139-157. doi:10.1016/s0169-409x(01)00112-0
60. Paxton N, Smolan W, Böck T, Melchels F, Groll J, Jungst T. Proposal to assess printability of bioinks for extrusion-based bioprinting and evaluation of rheological properties governing bioprintability. *Biofabrication*. 2017;9(4):044107. doi:10.1088/1758-5090/aa8dd8
61. Zidan A, Alayoubi A, Coburn J, et al. Extrudability analysis of drug loaded pastes for 3D printing of modified release tablets. *International Journal of Pharmaceutics*. 2019;554:292-301. doi:10.1016/j.ijpharm.2018.11.025
62. Allen LV. *Ansel's Pharmaceutical Dosage Forms and Drug Delivery Systems*. Philadelphia: Wolters Kluwer; 2018.
63. Lee K-J, Kang A, Delfino JJ, et al. Evaluation of Critical Formulation Factors in the Development of a Rapidly Dispersing Captopril Oral Dosage Form. *Drug Development and Industrial Pharmacy*. 2003;29(9):967-979. doi:10.1081/ddc-120025454
64. Dash S, Murthy PN, Nath L, Chowdhury P. Kinetic modeling on drug release from controlled drug delivery systems. *Acta Pol Pharm*. 2010;67(3):217-223.
65. Mathematical models of drug release. *Strategies to Modify the Drug Release from Pharmaceutical Systems*. 2015:63-86. doi:10.1016/b978-0-08-100092-2.00005-9